Volume 21
Number 17
7 May 2023
Pages 3467-3704

Organic & Biomolecular Chemistry

rsc.li/obc

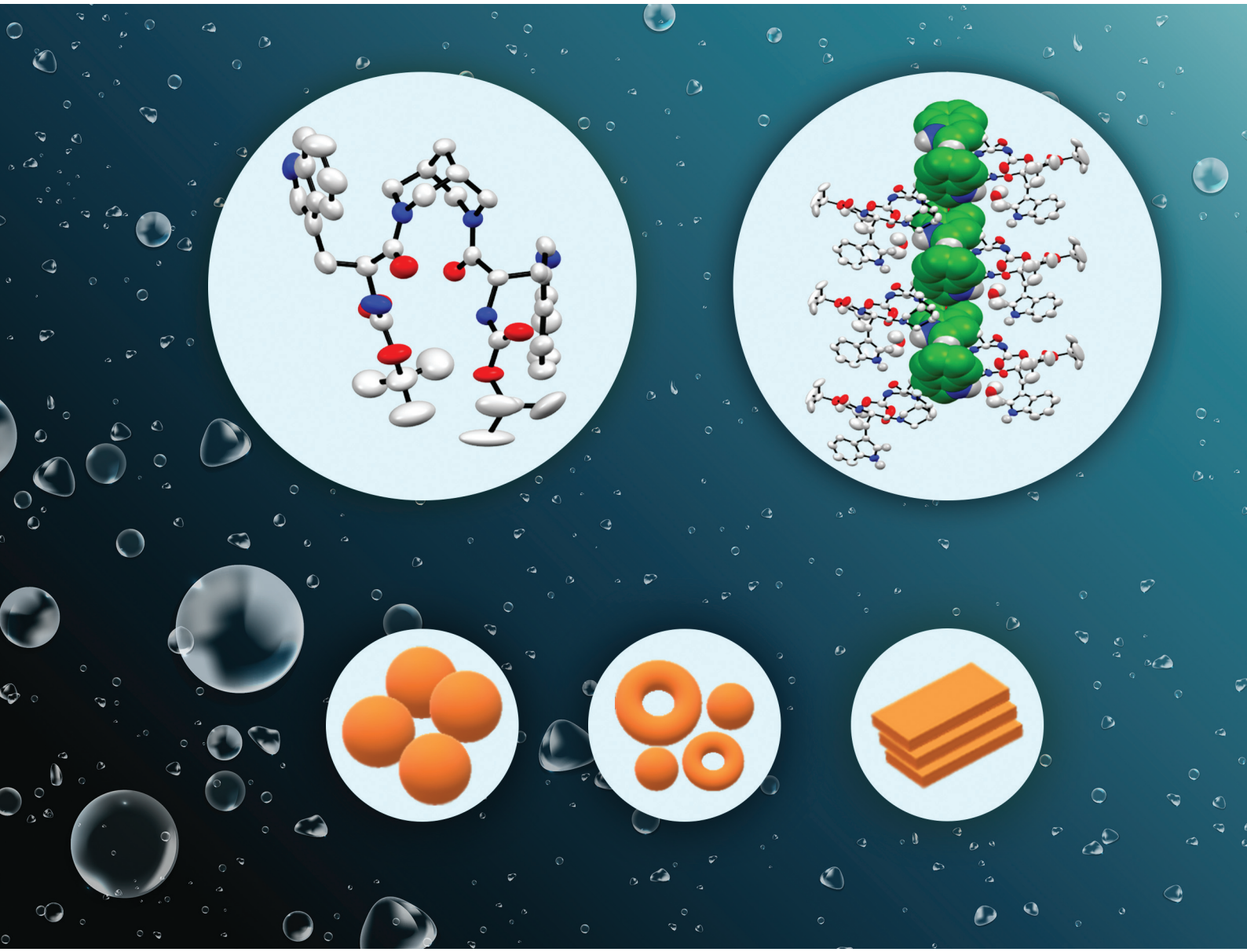

ISSN 1477-0520

ROYAL SOCIETY OF CHEMISTRY

PAPER

Aditya Mittal, V. Haridas *et al.*
Pseudopeptosomes: non-lipidated vesicular assemblies from bispidine-appended pseudopeptides

Organic & Biomolecular Chemistry

ROYAL SOCIETY OF CHEMISTRY

PAPER

View Article Online
View Journal | View Issue

Cite this: *Org. Biomol. Chem.*, 2023, **21**, 3557

Pseudopeptosomes: non-lipidated vesicular assemblies from bispidine-appended pseudopeptides†

Hanuman Singh, [a] Pragya Pragya,[b] Aditya Mittal *[b,c] and V. Haridas *[a]

Received 9th February 2023,
Accepted 17th February 2023

DOI: 10.1039/d3ob00201b

rsc.li/obc

We report a novel molecular topology-based approach for creating reproducible vesicular assemblies in different solvent environments (including aqueous) using specifically designed pseudopeptides. Deviating from the classical "polar head group and hydrophobic tail" model of amphiphiles, we showed (reversible) self-assembly of synthesized pseudopeptides into vesicles. Naming these new type/class of vesicles "pseudopetosomes", we characterized them by high-resolution microscopy (scanning electron, transmission electron, atomic force, epifluorescence and confocal) along with dynamic light scattering. While accounting for hydropathy index of the constituent amino acids (side chains) of pseudopeptides, we probed molecular interactions, resulting in assembly of pseudopeptosomes by spectroscopy (fourier-transform infrared and fluorescence). Molecular characterization by X-ray crystallography and circular dichroism revealed "tryptophan (Trp)-Zip" arrangements and/or hydrogen-bonded one-dimensional assembly depending on specific pseudopeptides and solvent environments. Our data indicated that pseudopeptosomes are formed in solutions by self-assembly of bispidine pseudopeptides (of Trp, leucine and alanine amino-acid constituents) into sheets that transform into vesicular structures. Thus, we showed that assembly of pseudopeptosomes utilizes the full spectrum of all four weak interactions essential in biological systems. Our findings have direct implications in chemical and synthetic biology, but may also provide a new avenue of investigations on origins of life *via* pseudopeptosome-like assemblies. We also showed that these designer peptides can act as carriers for cellular transport.

Introduction

Investigation of the formation of cell membranes from fundamental molecular building blocks has a unique place in contemporary scientific pursuits.[1,2] The "protocells" that might have formed in primordial conditions are believed to be the harbinger of life on Earth.[3] Therefore, development of a protocell model for studying and investigating innumerable issues in developmental biology is a challenging problem.

The building blocks of the early membrane of a protocell is not known. Therefore, the investigation of vesicular self-assembly from biologically relevant molecules such as peptides deserves special attention because the vesicular structure has a strong resemblance to the structure of primitive biological cells. A small molecule that assembles into a vesicular structure provides relevant clues on the origin-of-life problem.[4–6] Most vesicle-forming structures are based on a single-chain or double-chain lipidated amphiphiles.[7–9] Vesicles with a non-amphiphilic structure as part of the "primordial soup" have not been investigated.

Spherical vesicles are formed as a result of the spontaneous organization of molecules. Typically, the chemical structure of a vesicle-forming molecule consists of a charged head group and a long hydrocarbon tail. Phospholipids and sphingolipids are archetypical amphiphilic molecules that can assemble spontaneously into vesicles.[10] The chemical, physical, and biological aspects of vesicular assembly are being investigated because vesicles serve as prototypes of living cells. The lipophilic unit is present in the cell membrane as long lipid chains. These long lipid chains are conserved in the cell membrane, as well as the liposomes that we prepare in the laboratory.

The first example of a completely synthetic vesicular assembly was reported more than four decades ago.[11] Substantial efforts in this direction have been reported in the past decade.

[a]*Department of Chemistry, Indian Institute of Technology Delhi, Hauz Khas, New Delhi-110016, India. E-mail: haridasv@chemistry.iitd.ac.in*
[b]*Kusuma School of Biological Science, Indian Institute of Technology Delhi, Hauz Khas, New Delhi 110016, India. E-mail: amittal@bioschool.iitd.ac.in*
[c]*Supercomputing Facility for Bioinformatics, and Computational Biology (SCFBio), IIT Delhi, Hauz Khas, New Delhi 110016, India*

†Electronic supplementary information (ESI) available: Details on the synthesis and microscopy analysis and NMR experiments. CCDC 2172115 and 2172117. For ESI and crystallographic data in CIF or other electronic format see DOI: https://doi.org/10.1039/d3ob00201b

Formation of vesicular structures with different components, exhibiting "functional" features (*e.g.*, response to light),[12,13] environmental variables (*e.g.*, redox agents)[14,15] and pH[16,17] along with chemical interactions,[18] are opening up new avenues for exploring biomimicry. This work reports a vesicular assembly that we call a "pseudopeptosome", which is derived from the self-assembly of pseudopeptides. The latter have no structural similarity to "classical" amphiphiles.

The possibility of utilizing a lipophilic unit in structural formats other than a long lipid chain for vesiculation has not been investigated. We investigated the self-assembly of a series of pseudopeptides, wherein the hydrophobic part was in the form of a bicyclic unit reminiscent of a folded long chain, and the polar peptide bonds acted as the charged unit. Previously, we showed that the bispidine scaffold could nucleate the β-strand and β-arch.[19] Here, we report the ability of bispidine to induce vesiculation in organic and aqueous media. Moreover, these "designer peptides" can penetrate cells. Additionally, we demonstrated a "TrpZip" structure in the tryptophan (Trp)-appended compound.

The seven-carbon bicyclic structure (bispidine) was reminiscent of a seven carbon-long chain but folded into a compact "double chair" bispidine structure. These designer pseudopeptides containing lipophilic bispidine could penetrate cells. These bispidine-containing cell-penetrating pseudopeptides (CPPPs) were biocompatible according to the Resazurin assay.

We also demonstrated that our designer pseudopeptides assembled into bio-friendly pseudopeptosomes that had several potential applications. Interestingly, unlike phospholipid vesicular assemblies of size ~250 to ~1000 nm, which require 4000–80 000 molecular constituents,[20] our pseudopeptosomes of size ~500 nm showed many more molecular constituents (~10^8) with relatively "thicker" vesicular boundaries/walls. This indicated: (a) the involvement of more weak interactions towards vesicular stability; (b) possibly better control of the balance between morphological rigidity and flexibility in terms of more constituents from the perspective of law of mass-action governing self-assembly. Our design and synthesis of pseudopeptides, followed by their controlled assembly into novel vesicular structures called pseudopeptosomes, advances the scope of synthetic biology significantly, but may also open a new line of investigations towards various applications.

Results and discussion

Design and synthesis of pseudopeptides

Utilizing the tools of synthetic organic chemistry, but inspired by the utilization of naturally occurring molecules, we first explored creation of a lipophilic unit in non-phospholipidic structures. Thus, we created a series of pseudopeptides, wherein the hydrophobic part was in the form of a bicyclic unit (reminiscent of a folded long chain) and the polar peptide bonds acted as the charged unit. Fig. 1 shows examples of a seven-carbon system of a bicyclic structure. Clearly, it is unlike classical amphiphiles having a charged

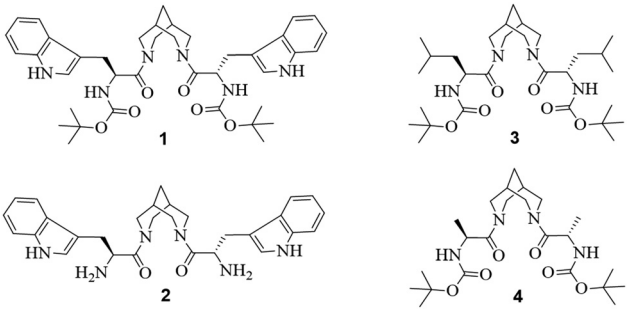

Fig. 1 Chemical structure of compounds **1–4**.

head group and one or two long (acyl or acyl-like) chains. Specifically, we chose the bicyclic unit bispidine as a spacer between two amino acids (Fig. 1). Compounds **1–4**, in which two amino-acid units are linked *via* a rigid bicyclic bispidine, were synthesized from Boc-protected piperidone, benzylamine, and formaldehyde through a double Mannich reaction, followed by Wolff–Kishner reduction of bispidinone.[21] The Boc- and benzyl-protected bispidine was converted to the designer systems **1–4** (Schemes S1 and S2†).

Pseudopeptosomes from a self-assembling pseudopeptide

To investigate the self-assembling properties of synthesized molecules, compound **1** was dissolved in methanol (1.43 mM) and the resulting assemblies analyzed by high-resolution microscopy (scanning electron microscopy (SEM), transmission electron microscopy (TEM) and atomic force microscopy (AFM)) (Fig. 2), along with dynamic light scattering (DLS). SEM images of **1** show spherical vesicular aggregates of

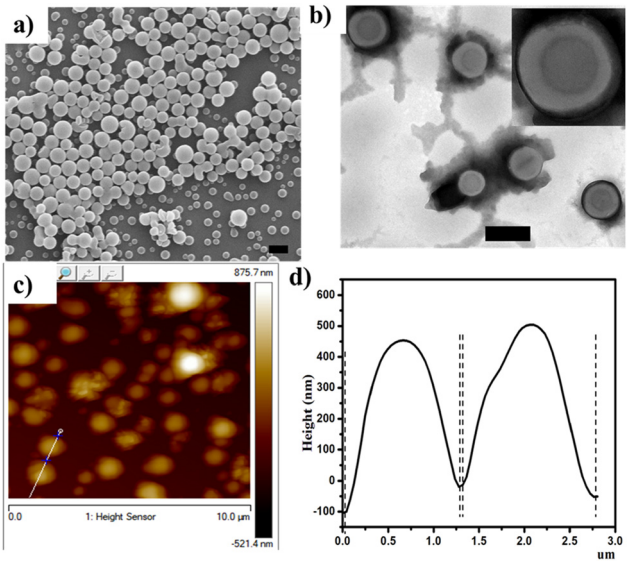

Fig. 2 Microscopic images of **1** (1 mg ml^{-1}) in methanol. (a) SEM, (b) TEM samples stained negatively using phosphotungstic acid for 1 min (inset shows clear contrast). (c) AFM. (d) Height profile of vesicles using AFM along the line shown in (c). The length of the scale bar is 1 μm.

size 200–1100 nm (Fig. 2a, Fig. S4a†). Concentration-dependent studies on **1** showed initial formation of sheets (Fig. S1a†), followed by toroid formation at a concentration of 0.715 mM (Fig. S1b†) and, on further increase in concentration, formation of vesicular assemblies (Fig. S1c†). Compound **1** also showed vesicular assembly in water : ethanol (1 : 1) (Fig. S1e†). A spherical "hollow" or "encapsulatable" nature of the formed vesicles on **1** was evident from TEM, which displayed a clear contrast in Fig. 2b and Fig. S2.† The volume of a hollow sphere is given by $V = (4/3\pi R^3 - 4/3\pi r^3)$, where R is the outer radius and r is the inner radius. TEM data showed R to be ~500 nm and r to be ~350 nm (Fig. S2†). Furthermore, the volume of one molecule of compound **1** (calculated from its crystal structure), V_{mol}, was ~1.5 nm × 1.5 nm × 1.5 nm = ~3.375 nm^3. Therefore, the number of molecules resulting in the observed vesicular self-assembly (*i.e.*, a pseudopeptosome) = $V/V_{mol} \sim 10^8$.

The critical aggregation concentration (CAC), which is analogous to the critical micellar concentration[22] and critical vesicular concentration,[23] of **1** was determined to be 175 μM based on DLS (Fig. S3b†). AFM imaging of **1** (Fig. 2c), while showing circular vesicles, also revealed the ratio of diameter : height larger than 1 : 1. However, as noted earlier,[24] sample preparations for AFM may result in flattening of spherical vesicles, presumably due to evaporation of the solvent from the vesicle and interaction with the surface. DLS studies of **1** revealed vesicle size to be 200–1100 nm (Fig. S3a†), which was consistent with AFM measurements (Fig. 2d) and SEM data (Fig. S3 and S4a†).

Pseudopeptosomes from different self-assembling pseudopeptides in different solvent environments

Next, the effect of bispidine on the nucleation of vesicular self-assembly with different amino acids and in different solvents was analyzed. Compounds **3** and **4** were synthesized to observe the effect of the "hydropathy index" of the amino acids (side chain) on self-assembly using SEM and epifluorescence microscopy (Fig. 3).

SEM of compounds **3** and **4** again showed vesicular assembly (Fig. 3a and b, Fig. S4c and d†) implying that bispidine plays a part in vesicular assembly rather than the hydropathy index of amino acids (*i.e.*, their side chains). The water-soluble compound **2** was also synthesized to see the solvent effect on the formation of vesicular assembly (Scheme S1†). Interestingly, compound **2** in water also formed vesicles of similar sizes (Fig. 3c) and the population of vesicles increased in 10% solution of methanol and water (Fig. S3†), which again showed that a bispidine scaffold had a significant role in forming the self-assembled structures. Compound **2** was a versatile molecule because it could form vesicles in methanol, water and mixture of water and methanol (Fig. 3c, Fig. S3†).

To obtain further insights into the mechanism of formation of vesicular assembly, fluorescence microscopy was undertaken using two "location-sensitive" measurements. Tryptophan (in compounds **1** and **2**) has fluorescence properties, but rhodamine B (RB) dye was chosen to probe the polar environment of vesicles.[25] Fig. 3d shows an epifluorescence microscopy image at 100× magnification (using Olympus IX51) of pseudopeptosomes formed by compound **1** but also carrying 0.02-equivalents of RB. Tryptophan fluorescence clearly showed a difference between fluorescence on the periphery and in the center of the vesicle.

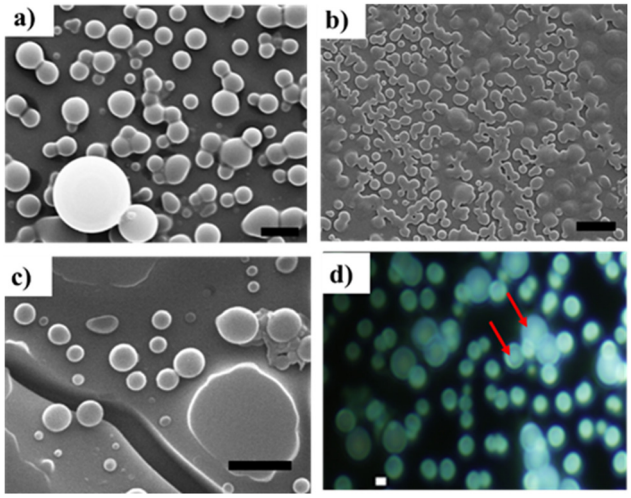

Fig. 3 (a) SEM image of **3**. (b) SEM image of **4**. (c) SEM image of **2**. (d) Epifluorescence microscopy image at 100× magnification of **1** + 0.02-equivalents of Rhodamine B dye at a UV filter. The length of the scale bar is 2 μm.

Pseudopeptosomes have biocompatible compartments

Confocal microscopy was used to overcome the observational limitations presented by epifluorescence microscopy. Targeted Z-optical sections (100 nm) were observed using specific laser sources for excitation (Fig. 4). Fig. 4a clearly shows RB to be encapsulated in the pseudopeptosomes formed by **1**. *Z*-stack analyses of the data from confocal fluorescence microscopy confirmed that RB was residing within pseudopeptosomes and was distributed uniformly in the three-dimensional environment (Fig. S5†). Confocal-based optical sectioning using specific laser based excitation had limited measurement capabilities for tryptophan fluorescence (due to the requirement for UV-region wavelengths), so we also used Nile Red (NR) dye to probe hydrophobic regions[25] of pseudopeptosomes. Confocal microscopy of NR-stained pseudopeptosomes, including their *Z*-stack analyses, showed NR on the periphery of pseudopeptosomes of **1** (Fig. 4b, Fig. S6†).

Interestingly, SEM data showed a slight increase in the vesicular sizes of **1** upon encapsulation with RB (Fig. S1d†). This result indicated the: (a) key roles of weak interactions in assembly of pseudopeptosomes similar to classical vesicular assemblies; (b) possibility of stoichiometric control of "cargo-dependent" size of pseudopeptosomes (but without any direct interaction with pseudopeptides, as demonstrated in subsequent results). Hence, we obtained conclusive evidence of pseudopeptosomes having appropriate compartments with hydrophobic shells encapsulating polar materials.

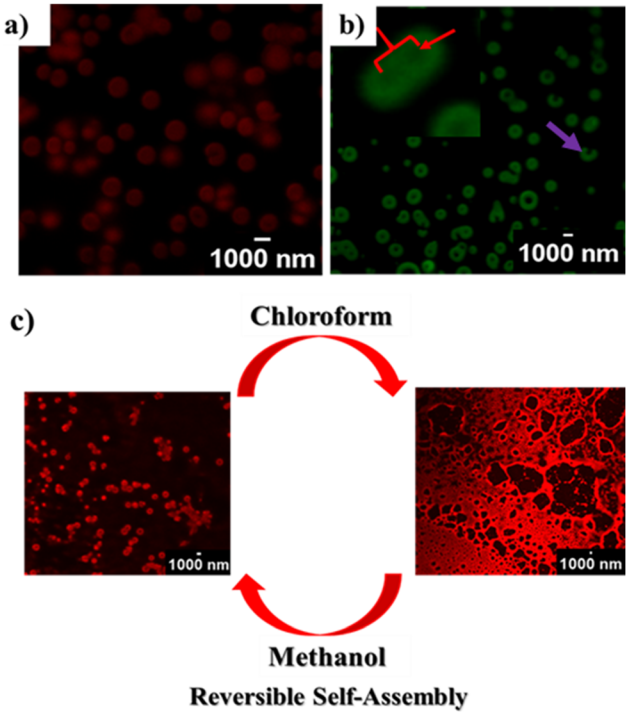

Fig. 4 (a) Confocal microscopic middle-frame image at 100× magnification (zoomed image) of **1** + 0.02-equivalents of Rhodamine B dye. (b) Confocal microscopic middle-frame image at 100× magnification (zoomed image) of **1** + 0.02-equivalents of Nile Red dye (inset shows vesicle fusion). (c) Reversible self-assembly of vesicles. Vesicles in methanol could be ruptured by adding chloroform, and rupture could be reversed by adding more methanol.

In addition, we also noted interesting vesicular properties of **1**, such as "fusion" and possible morphological transitions, as represented by fused vesicles and possible toroids (though the latter may have been a result from optical sectioning). These data showed that shells, despite being relatively thick, were also flexible. The expansion of vesicles in the presence of a guest such as RB indicates the plasticity of the vesicular assembly. RB molecules made several non-covalent interactions with the vesicle boundary, thereby leading to an enhancement in its size. Having confirmed the compartmental nature of pseudopeptosomes similar to those of classical vesicular assemblies, the biocompatibility of their constituents (*i.e.*, pseudopeptides) had to be tested. The cytotoxicity of compound **2** was studied by the Resazurin assay. RAW264.7 cells were treated with different concentrations (20–200 μg ml^{-1}) of compound **2** (prepared in serum-free media) for 24 h at 37 °C in an atmosphere of 5% CO_2. This was followed by incubation with 20 μl of resazurin (0.15 mg ml^{-1}) in 80 μl of serum-free media for 20 min at 37 °C in an atmosphere of 5% CO_2. Results (Fig. S7†) showed that compound **2** was non-toxic to cell viability at 0–200 μg ml^{-1}, thus establishing its biocompatibility.

To ascertain the potency of water-soluble pseudopeptide **2** as a delivery vehicle, intracellular uptake of RB in RAW264.7 cells was studied by confocal microscopy (Fig. S8†). RAW264.7 cells were treated with RB (5 μg ml^{-1}) along with **2** for 24 h. Confocal microscopy imaging indicated the cell-penetrating ability of pseudopeptide **2** (Fig. S8†) because RB was present within cells. A control experiment using RB alone revealed the inability of RB to penetrate cells.

To further expand the application of pseudopeptide **2**, we used a fluorescein isothiocyanate (FITC)-tagged peptide: corneal targeting sequence 1 (CorTS1). This peptide has been reported to have an activity against methicillin-resistant *Staphylococcus aureus* (MRSA) and *Fusarium dimerum*.[26]

We used two cargos (RB and CorTS1) and carried out a cell-uptake (monitored by measuring fluorescence using confocal microscopy) experiment in the presence of **2**. At a concentration of 10 μM, FITC fluorescence of CorTS1 peptide was not observed in cells (Fig. 5). However, when RAW264.7 cells were treated with CorTS1 mixed with pseudopeptide **2** (200 μg ml^{-1}) and RB (5 μg ml^{-1}), higher transport of CorTS1 to cells was noted. These results supported the notion of a cell-penetrating ability of pseudopeptide **2** and its ability to carry cargo.

We wished to obtain some mechanistic information on the self-assembly of our pseudopeptides into pseudopeptosomes. Fourier transform infrared (FT-IR) spectroscopy of compound **1** showed an intense band at 3418 cm^{-1} indicating non-hydrogen-bonded NHs. IR absorption bands at ~1634 cm^{-1} (amide I) revealed a β-strand arrangement (Fig. S9†).[27] A band at 1696 cm^{-1} also indicated β-strand structure. The chemical shift of $C_\alpha H$ of the amino acids in all compounds was moved downfield as compared with that of a random coil, thereby confirming a β-strand structure (Table S1†).[28]

Circular dichroism (CD) of compound **1** showed a negative band at 222 nm and positive bands at 232 nm and 205 nm (Fig. 6a). The band at 232 nm indicated interactions between the aromatic chromophores of tryptophan.[29–31] The negative band at ~222 nm indicated β-strand formation.[32,33]

The powder XRD (PXRD) patterns of compound **1** exhibited a reflection peak in the wide-angle region, which is characteristic of a typical π–π stacking distance ~3.35 Å (Fig. 6b), and indicated that hydrogen bonding and π–π stacking interactions were involved in vesicular self-assembly.[34] The CD spectrum of compound **2** showed a band at ~232 nm (which indicated interactions between the indole units of the Trp residue) (Fig. 6c) and a negative band at ~222 nm (which indicated β-strand formation). The CD spectra of compounds **3**[19] and **4** (Fig. 6c) also showed β-strand formation.[32,33]

The single-crystal X-ray structure of **1** (Fig. 7) also revealed a Trp-zip arrangement which supported the PXRD data. The crystal structure of **1** (Fig. 7a, Table S2†) showed bispidine in a chair–chair conformation, and two carbonyls are anti to each other. The anti-arrangement allowed the molecules to pack bidirectionally through hydrogen bonding. The indole NH of Trp hydrogen-bonded with neighboring molecules through the amide carbonyl, thereby forming a one-dimensional string (Fig. 7b). The other indole took part in hydrogen bonding with a carbonyl group of the neighboring molecule through a water molecule (Fig. 7c). The Trp involved in water-mediated hydrogen bonding further associated to form a Trp-zipper (Fig. 7d).

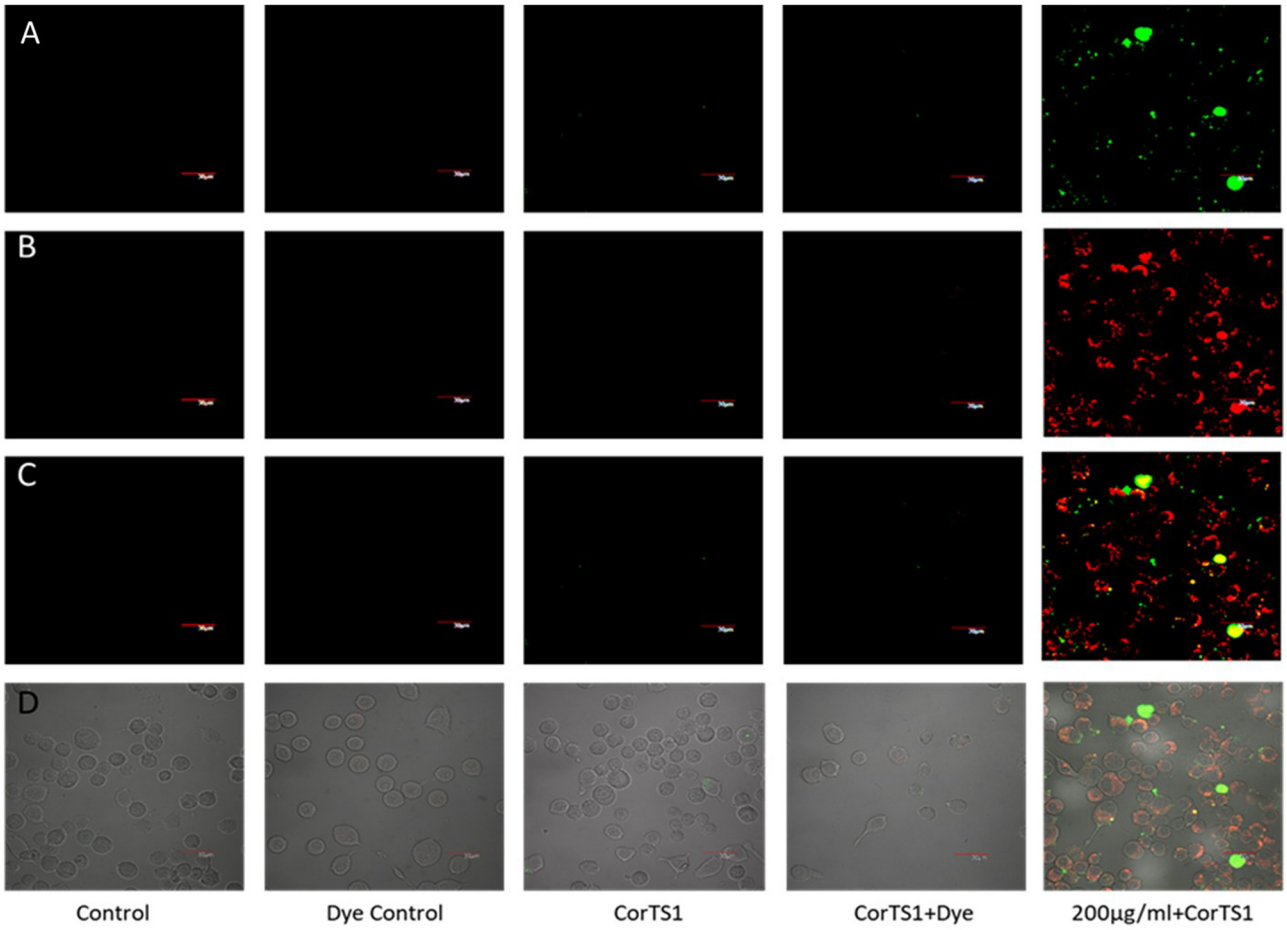

Fig. 5 Representative confocal microscopy images of RAW264.7 cells treated with CorTS1 and Rhodamine B along with compound **2**. Horizontal panels: (A) Fluorescence image of CorTS1. (B) Fluorescence image of Rhodamine B along with compound **2**. (C) Fluorescence merged images. (D) DIC-Fluorescence merged image. Vertical panels: (1) Control (cells only); (2) Dye control (cells incubated with Rhodamine B); (3) CorTS1 (cells incubated with CorTS1); (4) CorTS1 + Dye (cells incubated with Rhodamine B and CorTS1); (5) Cells incubated with Rhodamine B, CorTS1 and Compound **2**. Incubation was followed by washing with PBS and Imaging using an Olympus Confocal FV1200 microscope at 60× magnification (scale bar = 30 µm).

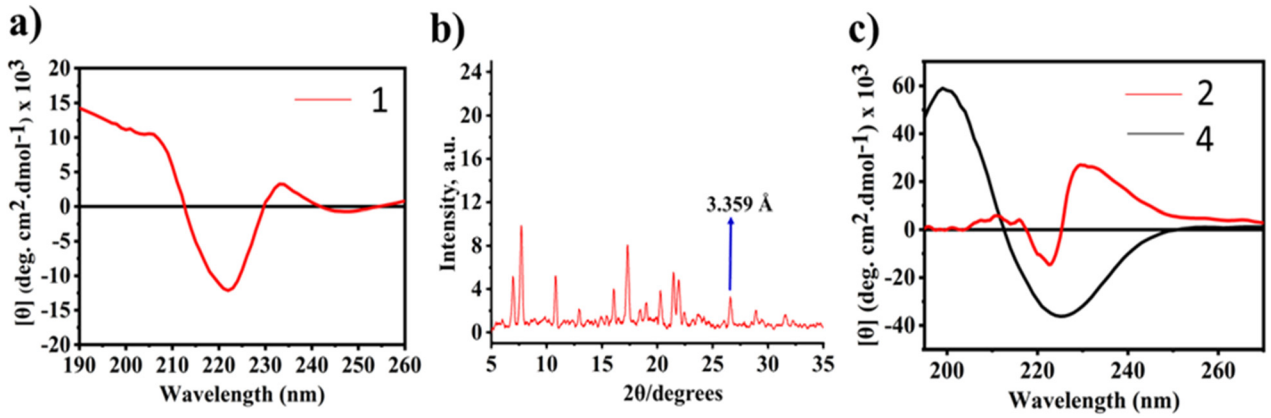

Fig. 6 (a) CD spectrum of **1**. (b) PXRD of **1** (blue arrow indicates distance of π–π interaction). (c) CD spectra of **2** and **4**.

The Leu-appended compound **3** was also crystallized from DMSO (Fig. 7e, Table S3†). The crystal structure reported here is very similar to that of a crystal from chloroform.[19] Compound **3** organized to a one-dimensional string through hydrogen bonding of amide (Fig. 7f and g). Despite subtle differences in the hydrogen bonds in **1** and **3**, both self-

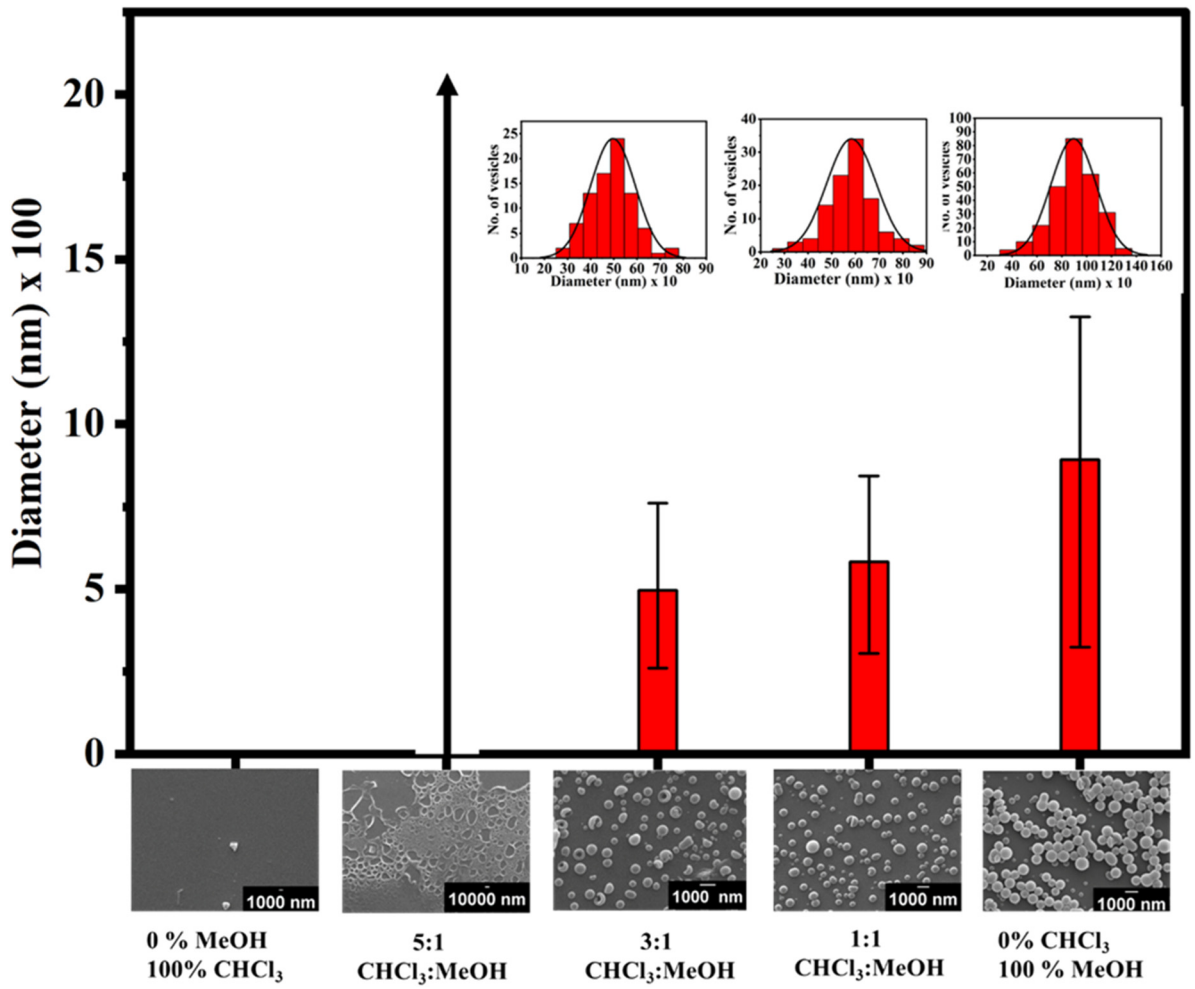

Fig. 8 Solvation effect on vesicular assembly. Different ratios of methanol and chloroform used for vesicle preparation. Insets indicate the size distribution of vesicles.

assembled to form vesicles in solution. The crystal structures of **1** and **3** suggested that both formed extended packing that became bent eventually to form vesicles. Interestingly, vesicles could be made from various amino acids containing peptides. The common feature in all of these peptides was bispidine, so it had a nucleating effect for vesicular assembly. The pseudopeptide design was versatile because it allowed for the design of vesicles in an organic solvent (organo-vesicles) in the case of **1** and aqueous-vesicles and organo-vesicles in the case of **2**. These vesicles were stabilized in polar solvents such as methanol and water.

A concentration-dependent nuclear magnetic resonance (NMR) study of **1** showed an upfield shift in aromatic protons and downfield shift in indole NH (Fig. S10†). These data supported the role of aromatic interactions and hydrogen bonding have important roles in vesicle formation. Thus, it appears that, as opposed to classical vesicular assemblies that rely on specific dominance of hydrophobic interactions operating only in aqueous solution, the pseudopeptosomes we prepared utilized the full spectrum of all four weak interactions that are essential in biological systems.

Considering that pseudopeptosomes are formed by self-assembly of pseudopeptides and utilize the full spectrum of the four weak interactions, we wanted to test them for reversible self-assembly in different solvents. The removal/addition of chloroform in the solvent environment of compound **1** was carried out. Remarkably, Fig. 4c shows the solvent-dependent reversibility of pseudopeptosome formation of **1** as observed by confocal microscopy. The reversible behavior in pseudopeptosome assembly allows exploration of applicational avenues such as creation of reversible sub-micron reaction centers.

Solvation effects the assembly of pseudopeptosomes

Inspired by the discovery of the solvent-dependent reversible vesicular self-assembly of **1**, we carried out detailed high-resolution microscopy studies to test the effects of polar/non-polar environments on vesicular assembly of compound **1**. The effects of varying the solvent environment created by titrating

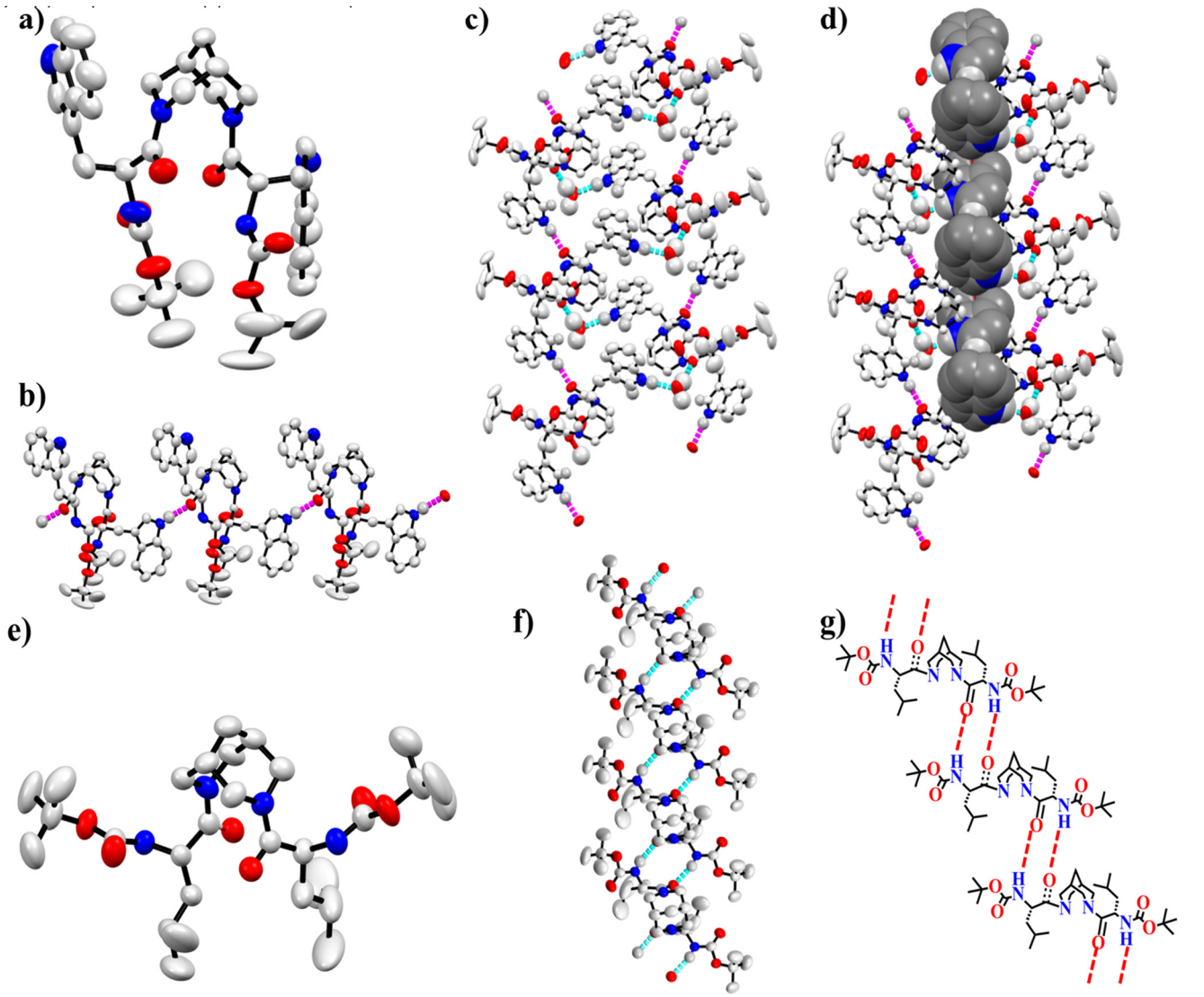

Fig. 7 (a) and (e) are the X-ray crystal structures of **1** and **3** with a 50% probability level of atomic displacement ellipsoids. (b) One dimensional extended structures of **1** showing hydrogen bonding between carbonyl oxygen and indole ring of one Trp unit (purple). (c) Indole ring of the Trp unit takes part in hydrogen bonding to the carbonyl group of the neighboring molecule through a water molecule (cyan). (d) The Trp-Zip arrangement mediated by C–H···π interaction (spacefill model) between the π-system of Trp and C–H from neighboring indole (distance = 2.87 Å and angle = 157.2°). (f) One-dimensional stringing amide hydrogen bonding. (g) Structural representation of amide hydrogen bonding in **3** observed in the solid state.

methanol and chloroform on pseudopeptosome formation are shown in Fig. 8. Vesicular assemblies were not observed in pure chloroform, but methanol : chloroform at 1 : 5 favored vesicular formation. Furthermore, methanol : chloroform at 3 : 1 shoor partially form/or partially formed vesicles.[35,36] Complete vesicles were formed in methanol : chloroform at 1 : 1. An increase in the percentage of methanol resulted in an increase in vesicle size (Fig. 8). These results clearly showed that methanol favoured, whereas chloroform disrupted, vesicular assembly.

Diffusion ordered spectroscopy (DOSY) of compound **1** at different concentrations in methanol showed that diffusion-coefficient values decreased upon increasing concentration (Fig. S11†) and that the diffusion coefficient in chloroform : methanol at 1 : 1 was lower compared with that of chloroform solution (Fig. S12†), again confirming self-assembly in methanol (molecules of compound **1** were expected to show a lower diffusion coefficient in self-assembled forms compared with being free).

Fluorescence spectroscopy showed that the intrinsic fluorescence of compound **1** at 339 nm first increased until 0.130 mM (Fig. S13a†), and then fluorescence was quenched upon increasing the concentration (Fig. S13b and S13c†). Interestingly, the concentration at which quenching was observed was equivalent to the CAC calculated by DLS (Fig. S3†). Addition of 0.02-equivalent of RB to compound **1**

(λ_{ex} 553 nm) showed no significant changes in dye emission, indicating that RB did not interact with tryptophan (Fig. S13d†).

Three models can be proposed for vesicle formation. In model I (Fig. 9a(i)), the hydrophobic part forms the interface and the hydrophilic part is exposed to the inside and outside of the vesicle. In model II (Fig. 9a(ii)), hydrophobic regions are exposed to inside and outside of the vesicle. In a polar solvent, model I is probably favored. The thickness of the vesicle wall supports a multilayer arrangement (model III) (Fig. 9a(iii) and b). Hence, model III is most preferred in our system.

The self-assembly of **1** is influenced by the concentration and solvent system. At 0.35 mM, morphology is a sheet. At 0.72 mM, morphology is half-toroids and toroids, and vesicles are observed mainly at 1.43 mM. Similarly, methanol favors vesicles, while chloroform does not favor vesicular assembly, as shown in the phase diagram (Fig. 9c).

The anion-sensing property of compound **1** was also investigated with $H_2PO_4^-$, F^-, Br^-, HSO_4^- and I^- as their TBA salts. An excellent TURN ON fluorescence was observed upon the addition of some anions (Fig. S14a†), while such changes were not prominent with other anions. Among all anions (F^-, Cl^-, Br^-, I^-, HSO_4^-, $H_2PO_4^-$) tested, only F^- and $H_2PO_4^-$ caused maximum fluorescence enhancement. Binding of $H_2PO_4^-$ resulted in a 17 nm red-shift in fluorescence maxima. Job plots showed a 1 : 1 stoichiometry (Fig. S14b†). These results indicated that, while pseudopeptides designed and created by us assembled into pseudopeptosomes, they also have the potential to be developed into sensors.

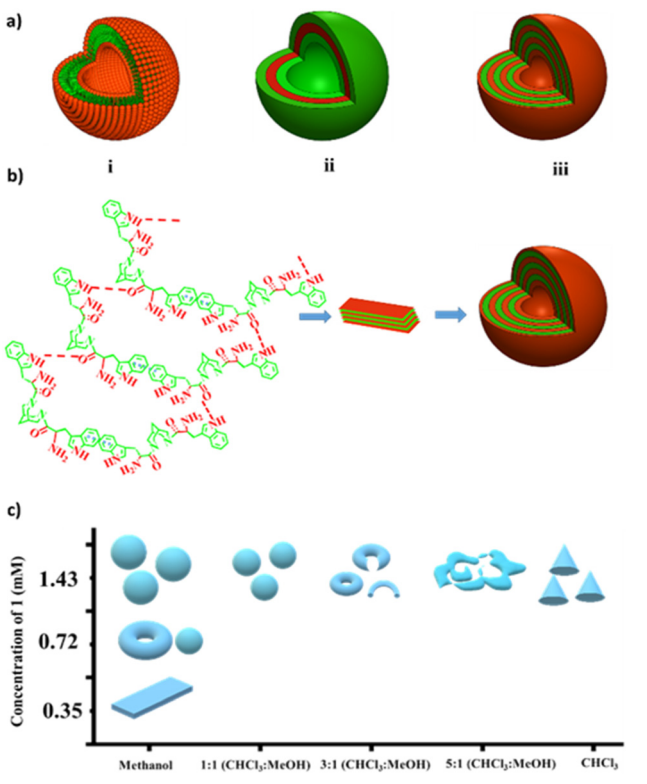

Fig. 9 (a) Graphical representation of different types of vesicular assemblies. (i) Classical model I. (ii) Proposed reverse bilayer model II. (iii) Proposed multilayer model III. Red and green parts represent hydrophilic and hydrophobic groups, respectively. (b) Proposed assembly of **2** based on the crystal structure of **1** supports the proposed model III (multilayer vesicles). (c) Phase diagram representing the role of concentration and solvent composition on the self-assembly of **1**. Cone shape represents a compound molecularly dispersed in solution.

Conclusions

In general, it is thought that vesicular assemblies, mimicking biological cells and subcellular compartments, are formed due to the hydrophobically-driven self-assembly of amphiphilic molecules in aqueous environments.[22,37–40] At the same time, manifestations of biological functions result from the action of polymeric structures (predominantly proteins) within particular ranges of environmental variables.[41,42] Vesicular assemblies utilize the full spectrum of four weak interactions (hydrogen-bonding, ionic interactions, van der Waals forces and hydrophobic interactions). Clearly, a balance between maintaining morphological rigidity *vs.* flexibility along with retention of reversible vesicular self-assembly is a hallmark of molecular assemblies relevant to biological systems. We took inspiration from: (a) amino acids as building blocks of proteins that allow a myriad of functional structures realized through various physicochemical interactions; (b) amphiphilic assemblies resulting in the formation of whole cells and subcellular compartments; (c) molecular topology-based concepts found in biological assemblies[43,44] and protein folding.[23,45,46] Our molecular-topology based design of pseudopeptides, with amino acids appended on rigid bispidine, deviates from the classical "polar head group and hydrophobic tail" model of amphiphiles. Providing net polarity to one part of a designer molecule by orienting dipoles within structures that have inherent carbon–chain arrangements for hydrophobicity obviates the need for a separate "polar head" or "long tails" for vesicular self-assembly. We described vesiculation in pseudopeptides containing three amino acids (Ala, Leu, and Trp). This design allowed fabrication of vesicles in organic and aqueous solutions. More importantly, controllable formation of pseudopeptosomes allowed full exploration of all possible weak interactions in self-assembling systems rather than relying heavily on just one *vs.* the other. For example, pseudopeptosomes formed by compound **1** in MeOH and MeOH : water at 1 : 1 indicated that hydrophobic interactions were not the predominant mode of vesicular assembly, implying that an entropy-driven process was not the favored one. Addition of MeOH favored hydrogen-bonding, hence implying an enthalpy-driven assembly. The hydrogen bond-assisted "sheets" eventually became curved (possibly due to other weak interactions, including hydrophobicity), resulting in vesicles. Important parts were also played by other local interactions, such as Trp-zippers.[47] Thus, we showed that a combination of dipoles and hydrophobic parts in molecular entities (and not just charged units and long-chain hydrocarbons) could be generic struc-

tural requirements for molecules self-assembling into vesicles. Our work has direct relevance to chemical and synthetic biology, and also provides applicational ideas for designing biocompatible delivery vehicles.

Author contributions

VH conceived the study. VH and AM designed experiments and assisted in data analyses. HS participated in designing experiments, carried out the experiments, collected the data, prepared the figures and analyzed the data. PP assisted in carrying out epifluorescence and confocal-microscopy experiments as well as carrying out cytotoxicity studies, collecting and analyzing relevant data. HS, VH and AM wrote the final version of the manuscript with input from PP.

Data availability

All synthetic procedures, microscopic analysis, and NMR data supporting this article are in the ESI.†

Conflicts of interest

There are no conflicts to declare.

Acknowledgements

VH is grateful to the Department of Science and Technology, Government of India, for support. HS thanks the Council of Scientific and Industrial Research, New Delhi, for a fellowship. PP thanks University Grants Commission, New Delhi, for a fellowship. AM is grateful for financial support from the Kusuma Trust (UK), which allowed him to establish the confocal-microscopy facility at IIT Delhi. The authors are grateful to the Department of Chemistry, Central Research Facility, and the Kusuma School of Biological Sciences at IIT Delhi. We thank Upanshu Gangwar for helping in DOSY NMR experiments. We thank Professor Archana Chugh for providing the FITC-labelled peptide.

References

1 N. Kitadai and S. Maruyama, *Geosci. Front.*, 2018, **9**, 1117–1153.
2 M. Frenkel-Pinter, M. Samanta, G. Ashkenasy and L. J. Leman, *Chem. Rev.*, 2020, **120**, 4707–4765.
3 J. P. Schrum, T. F. Zhu and J. W. Szostak, *Cold Spring Harbor Perspect. Biol.*, 2010, **2**, a002212–a002212.
4 V. Haridas, *Acc. Chem. Res.*, 2021, **54**, 1934–1949.
5 V. Luis and I. Alfonso, *Acc. Chem. Res.*, 2014, **47**, 112–124.
6 C. Wanzke, A. Jussupow, F. Kohler, H. Dietz, V. R. I. Kaila and J. Boekhoven, *ChemSystemsChem*, 2020, **2**, e190004.
7 D. W. P. M. Löwik and J. C. M. van Hest, *Chem. Soc. Rev.*, 2004, **33**, 234–245.
8 S. F. Jordan, H. Rammu, I. N. Zheludev, A. M. Hartley, A. Maréchal and N. Lane, *Nat. Ecol. Evol.*, 2019, **3**, 1705–1714.
9 R. J. Brea, A. Bhattacharya, R. Bhattacharya, J. Song, S. K. Sinha and N. K. Devaraj, *J. Am. Chem. Soc.*, 2018, **140**, 17356–17360.
10 A. Bhattacharya, R. J. Brea, H. Niederholtmeyer and N. K. Devaraj, *Nat. Commun.*, 2019, **10**, 300.
11 T. Kunitake and Y. Okahata, *J. Am. Chem. Soc.*, 1977, **99**, 3860–3861.
12 S. K. M. Nalluri and B. J. Ravoo, *Angew. Chem., Int. Ed.*, 2010, **49**, 5371–5374.
13 C. Park, J. Lim, M. Yun and C. Kim, *Angew. Chem., Int. Ed.*, 2008, **47**, 2959–2963.
14 W. Ong, Y. Yang, A. C. Cruciano and R. L. McCarley, *J. Am. Chem. Soc.*, 2008, **130**, 14739–14744.
15 A. Napoli, M. Valentini, N. Tirelli, M. Müller and J. A. Hubbell, *Nat. Mater.*, 2004, **3**, 183–189.
16 J. Du and S. P. Armes, *J. Am. Chem. Soc.*, 2005, **127**, 12800–12801.
17 J. Du, Y. Tang, A. L. Lewis and S. P. Armes, *J. Am. Chem. Soc.*, 2005, **127**, 17982–17983.
18 K.-D. Zhang, G.-T. Wang, X. Zhao, X.-K. Jiang and Z.-T. Li, *Langmuir*, 2010, **26**, 6878–6882.
19 H. Singh, A. Chenna, U. Gangwar, J. Borah, G. Goel and V. Haridas, *Chem. Sci.*, 2021, **12**, 15757–15764.
20 J. Bentz, S. Nir and J. Wilschut, *Colloids Surf.*, 1983, **6**, 333–363.
21 V. Haridas, S. Sadanandan, M. V. S. Gopalakrishna, M. B. Bijesh, R. P. Verma, S. Chinthalapalli and A. Shandilya, *Chem. Commun.*, 2013, **49**, 10980.
22 C. Tanford, *The hydrophobic efect: formation of micelles and biological membranes*, Wiley, New York, 1973.
23 A. Mittal and R. Grover, *J. Nanosci. Nanotechnol.*, 2010, **10**, 3085–3090.
24 M. Yang, W. Wang, F. Yuan, X. Zhang, J. Li, F. Liang, B. He, B. Minch and G. Wegner, *J. Am. Chem. Soc.*, 2005, **127**, 15107–15111.
25 C. Berkland, E. Pollauf, N. Varde, D. W. Pack and K. K. Kim, *Pharm. Res.*, 2007, **24**, 1007–1013.
26 S. Shankar, S. G. Shah, S. Yadav and A. Chugh, *Eur. J. Pharm. Biopharm.*, 2021, **166**, 216–226.
27 A. Dong, P. Huang and W. S. Caughey, *Biochemistry*, 1990, **29**, 3303–3308.
28 D. S. Wishart, B. D. Sykes and F. M. Richards, *Biochemistry*, 1992, **31**, 1647–1651.
29 A. G. Cochran, N. J. Skelton and M. A. Starovasnik, *Proc. Natl. Acad. Sci. U. S. A.*, 2001, **98**, 5578–5583.
30 L. Wu, D. McElheny, R. Huang and T. A. Keiderling, *Biochemistry*, 2009, **48**, 10362–10371.
31 I. B. Grishina and R. W. Woody, *Faraday Discuss.*, 1994, **99**, 245.
32 D. E. Clarke, E. T. Pashuck, S. Bertazzo, J. V. M. Weaver and M. M. Stevens, *J. Am. Chem. Soc.*, 2017, **139**, 7250–7255.
33 L. Zhai, Y. Otani, Y. Hori, T. Tomita and T. Ohwada, *Chem. Commun.*, 2020, **56**, 1573–1576.

34 K. Aoki, M. Nakagawa and K. Ichimura, *J. Am. Chem. Soc.*, 2000, **122**, 10997–11004.
35 A. R. Sapala, J. Kundu, P. Chowdhury and V. Haridas, *New J. Chem.*, 2016, **40**, 9907–9911.
36 V. Haridas, M. B. Bijesh, A. Chandra, S. Sharma and A. Shandilya, *Chem. Commun.*, 2014, **50**, 13797–13800.
37 A. Mittal, A. M. Changani and S. Taparia, *J. Biomol. Struct. Dyn.*, 2020, **38**, 4579–4583.
38 C. Tanford, *Science*, 1978, **200**, 1012–1018.
39 A. Mittal and A. Chauhan, *J. Membr. Biol.*, 2022, **255**, 185–209.
40 T. Baumgart, S. T. Hess and W. W. Webb, *Nature*, 2003, **425**, 821–824.
41 K. Ghosh and K. Dill, *Biophys. J.*, 2010, **99**, 3996–4002.
42 K. A. Dill, K. Ghosh and J. D. Schmit, *Proc. Natl. Acad. Sci. U. S. A.*, 2011, **108**, 17876–17882.
43 J. N. Israelachvili, D. J. Mitchell and B. W. Ninham, *J. Chem. Soc., Faraday Trans. 2*, 1976, **72**, 1525.
44 S. Bansal and A. Mittal, *J. Membr. Biol.*, 2013, **246**, 557–570.
45 A. Mittal and B. Jayaram, *J. Biomol. Struct. Dyn.*, 2011, **28**, 443–454.
46 A. Mittal and B. Jayaram, *J. Biomol. Struct. Dyn.*, 2011, **28**, 669–674.
47 V. Haridas, S. Sadanandan, S. Dhawan, R. Mishra, I. Jain, G. Goel, Y. Hu and S. Patel, *Org. Biomol. Chem.*, 2017, **15**, 1661–1669.

Electronic Supplementary Information

Pseudopeptosomes: Non-lipidated vesicular assemblies from bispidine appended pseudopeptides

Hanuman Singh,[a] Pragya Pragya,[b] Aditya Mittal,*[b,c] V. Haridas,*[a]

[a]Department of Chemistry, Indian Institute of Technology Delhi, Hauz Khas, New Delhi 110016, India

*E-mail: haridasv@chemistry.iitd.ac.in (ORCID ID: 0000-0002-2931-0585)

[b]Kusuma School of Biological Science, Indian Institute of Technology Delhi, Hauz Khas, New Delhi 110016, India

[c] Supercomputing Facility for Bioinformatics, and Computational Biology (SCFBio), IIT Delhi, Hauz Khas, New Delhi 110016, India

*E-mail: amittal@bioschool.iitd.ac.in (ORCID ID: 0000-0002-4030-0951)

*Correspondence

Experimental method

All the chemical reactions were performed in oven-dried glassware. Reagents used in our experiments were purchased from Sigma-Aldrich and Alfa Aesar (India). Standard drying methods were employed for solvents used in reactions. Silica gel thin-layer chromatography(TLC) was used to monitor all reactions. Compounds were purified by silica gel (100−200 mesh) column chromatography using ethyl acetate/hexane as the eluent. Infrared spectra were recorded as KBr pellets using a Perkin Elmer FT-IR/FIR Spectrometer Frontier. ^{1}H and ^{13}C NMR spectra were recorded on a Bruker 300, 400, and 500MHz spectrometers. The NMR chemical shifts were reported relative to tetramethylsilane as the reference. Circular Dichroism (CD) spectra were recorded on AVIV model 410 spectropolarimeter. A 1mm path length of cuvette was used to record CD spectra. Mass spectra (HRMS) were recorded in a Bruker MicrO-TOF-QII model using ESI technique. Melting points were recorded on a Fisher scientific melting point apparatus. High-performance liquid chromatography (HPLC), Shimadzu (Model CBM-20A) was used. Optical rotations were measured with a Rudolph Research Analytical Autopol® V Polarimeter. The concentrations were reported in gram/100mL. X-ray diffraction analysis was carried out on a BRUKER AXS SMARTAPEX diffractometer with a CCD area detector (Mo Kα = 0.71073Å, monochromator: S3 graphite). Structure solution, refinement, and data output were carried out with the ShelXTL program. Powder X-Ray diffraction (PXRD) pattern were taken on Bruker D8 Advance diffractometer using Ni-filtered Cu Kα radiation.

Synthetic schemes

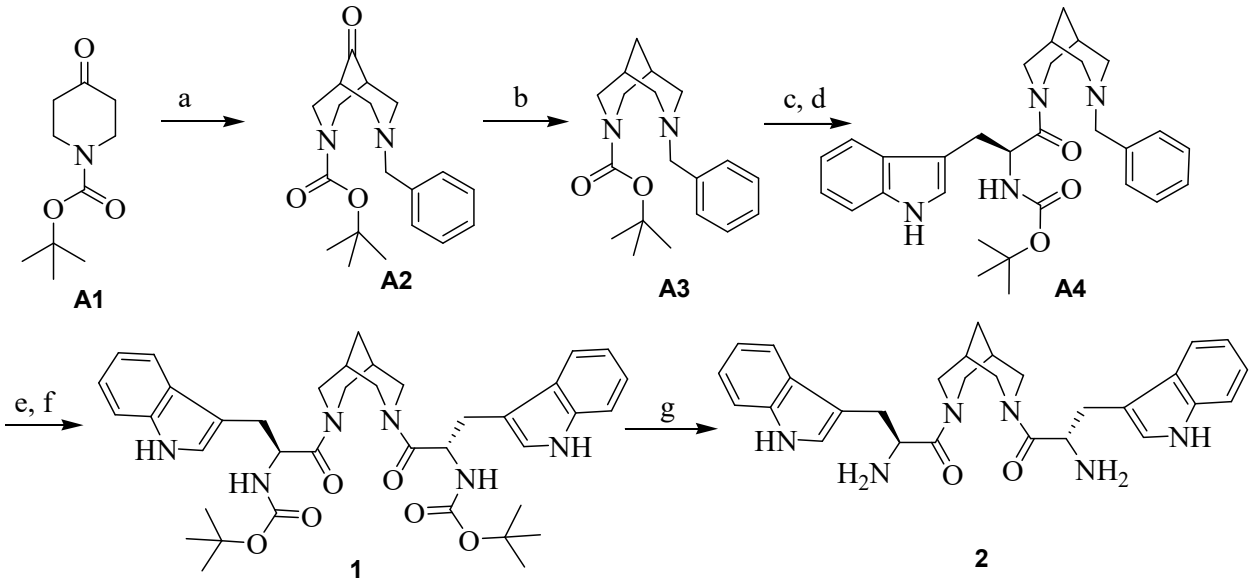

Reagents: (a) Benzyl amine, HCHO, AcOH, MeOH, 65 ºC, 10 h, 60%; (b) NH_2NH_2, Glycol, KOH, 8 h,165 ºC, 85%; (c) TFA, DCM, 4 h at RT; (d) Boc-Trp-OH, DCC, NHS, DCM, NEt_3, 24 h at RT; (e) 10% of Pd/C, MeOH, AcOH, 8 h at RT; (f) Boc-Trp-OH, DCC, NHS, DCM, NEt_3, 24 h, at RT; (g) EtOAc.HCl.

Scheme S1. Synthesis of **1**.

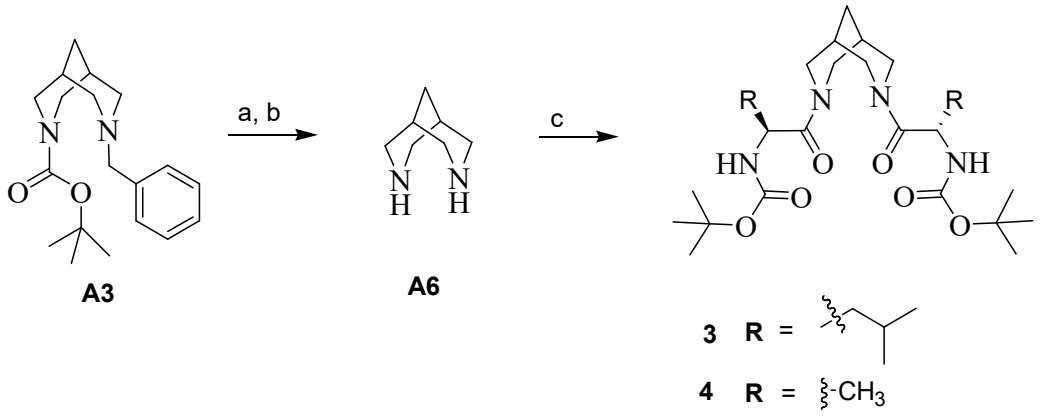

Reagents: (a) 10% of Pd/C, MeOH, AcOH, 8 h at RT; (b) TFA, DCM, 4 h at RT; (c) Boc-Leu-OH or Boc-Leu-OH, DCC, NHS, DCM, NEt_3, 24 h at RT.

Scheme S2. Synthesis of **3** and **4**.

Synthesis of **1**

To a well stirred solution of compound **A4**[1] (0.438 g, 0.87 mmol) in methanol was added few drops of acetic acid and 10% of Pd/C (0.043 g) and the solution was kept under positive pressure of H_2 gas. Stirred the reaction mixture for 8 h under H_2 at room temperature. The reaction mixture was filtered and the filtrate was evaporated in *vacuo*. The amine obtained was then added to the dichloromethane (DCM) solution of tert-butyloxy carbonyl (Boc) protected tryptophan (0.221 g, 0.72 mmol), N-Hydroxysuccinimide (NHS) (0.099 g, 0.86 mmol), N,N′-Dicyclohexylcarbodiimide (DCC) (0.177 g, 0.86 mmol) and triethylamine (NEt_3) (0.4 mL, 2.88 mmol). The solution was stirred for 24 h at room temperature and monitored by thin layer chromatography (TLC). After completion of the reaction, the mixture was evaporated and re-dissolved in ethyl acetate. The ethyl acetate part was washed with 0.2N H_2SO_4, saturated aq. $NaHCO_3$ and water. The organic layer was collected and dried over anhyd. Na_2SO_4 and evaporated under vacuum to obtain the crude product, which was purified by column chromatography (Ethyl acetate/Hexane in 4:6) to give 0.400 g compound **1** as a solid.

Yield: 78.8%

Mp: 172-174 ºC

$[\alpha]_D^{21}$ = -12º (c 0.05, methanol);

^{1}H NMR (300 MHz, $CDCl_3$) δ 1.28 (m, 2H), 1.42 (m, 2H), 1.56 (s, 18H), 1.79 (d, *J* = 12.9 Hz, 2H), 2.12 (d, *J* = 13.8 Hz, 2H), 2.92-3.28 (m, 4H), 3.47 (d, *J* = 12.9 Hz, 2H), 4.40 (d, *J* = 13.5 Hz, 2H), 4.88 (m, 2H), 5.90 (d, *J* = 7.5 Hz, 2H), 6.94 (m, 2H), 7.00 – 7.25 (m, 4H), 7.32 (d, *J* = 8.1 Hz, 2H), 7.57 (d, *J* = 7.5 Hz, 2H), 8.53 (br s, 2H); ^{13}C NMR (75 MHz, $CDCl_3$) δ 27.8, 28.26, 28.35, 28.7, 30.9, 31.5, 45.3, 49.7, 51.1, 79.6, 110.8, 111.0, 119.0, 119.2, 121.6, 123.1, 127.7,

136.0, 155.7, 170.6; IR (KBr): 3418, 2976, 2927, 2863, 1696, 1635, 1496, 1456, 1392, 1366, 1250, 1235, 1169; HRMS calcd. for $C_{39}H_{50}N_6O_6Na$ m/z 721.3684, found m/z 721.3704.

Synthesis of **2**

To **1** (0.150 g, 0.21 mmol) was added ethyl acetate saturated with HCl gas (10ml) in ice cold condition. The reaction mixture was stirred for 4 h at room temperature. The reaction mixture was evaporated and washed thrice with pentane to obtain 0.107 g of **2** as white solid.

Yield: Quantitative.

Mp: 240 -242 ^oC;

$[\alpha]_D^{21}$ = + 60^o (c 0.05, methanol);

^1H NMR (500 MHz, CD_3OD) δ 1.55 (br s, 2H), 1.72 (br s, 2H), 2.24 (d, *J* = 13 Hz, 2H), 2.33 (d, *J* = 13.5 Hz, 2H), 3.20 (dd, *J* = 9.5, 9 Hz, 4H), 3.35 (m, 2H), 3.76 (d, *J* = 13.5 Hz, 2H), 4.33 (d, *J* = 14 Hz, 2H), 4.88 (m, 2H), 7.04 (t, *J* = 7.5 Hz, 2H), 7.13 (t, *J* = 7.5 Hz, 2H), 7.19 (m, 2H), 7.38 (d, *J* = 8 Hz, 2H), 7.42 (d, *J* = 8 Hz, 2H); ^{13}C NMR (125 MHz, CD_3OD) δ 27.0, 29.2, 31.0, 45.4, 50.8, 50.9, 106.2, 111.2, 117.4, 118.9, 121.5, 124.1, 126.9, 136.6, 168.8; IR (KBr): 3402, 2922, 2866, 1634, 1491, 1457, 1343, 1243, 1100; HRMS calcd. for $C_{29}H_{35}N_6O_6$ m/z 499.2816, found m/z 499.2800.

Synthesis of **3**

To a well stirred solution of Boc and benzyl protected bispidine compound **A3** (0.295 g, 0.935 mmol) in methanol (10 mL) was added few drops of acetic acid and 10% of Pd/C (0.029 g) and kept under positive pressure of H_2 gas. Stirred the reaction mixture for 8 h at room temperature. The reaction mixture was filtered and evaporated in *vacuo* to obtain the amine. The obtained amine

was dissolved in DCM and trifluoroacetic acid (0.715 mL, 9.35 mmol), stirred for 2 h at room temperature. The reaction mixture was evaporated and used as such for further reaction. The obtained amine was added to the DCM solution containing tert-butyloxy carbonyl (Boc) protected leucine (0.432 g, 1.87 mmol), NHS (0.258 g, 2.24 mmol), DCC (0.460 g, 2.24 mmol) and NEt_3 (0.31 mL, 2.24 mmol). The resultant solution was stirred for 24 h at room temperature. After completion of reaction, the reaction mixture was evaporated and re-dissolved in ethyl acetate and the filtrate was washed with 0.2N H_2SO_4, saturated aq. $NaHCO_3$ and water. The organic part was dried over anhyd. Na_2SO_4 and evaporated under vacuum to obtain the crude product, which was purified by column chromatography (Ethyl acetate/Hexane in 4:6) to give 0.450 g compound **3** as a solid.

In the ^{1}H NMR spectrum in $CDCl_3$, compound **3** showed signals for major and minor conformers. We have mentioned the signals for minor conformer, wherever possible.^{13}C NMR also showed signal for minor conformer, which is also included in the data which leads to increased number of signals.

Yield: 87%. Mp: 156 -158 ^{o}C;

$[\alpha]_D^{21}$ = -88^o (c 0.05, methanol);

^{1}H NMR ($CDCl_3$, 500MHz): δ 0.88 (d, *J* = 6.5 Hz, minor), 0.93 (d, *J* = 7 Hz, 6H), 0.95 (d, *J* = 6.5 Hz, minor), 1.02 (d, *J* = 6.5 Hz, 6H), 1.16 (m, minor), 1.28 (m, 4H), 1.40 (s, 18H), 1.50 (s, minor), 1.63 (m, minor), 1.69 (m, 2H), 1.87 (br s, 2H), 1.90 (s, minor), 1.99 (s, minor), 2.12 (br s, 2H), 2.84 (d, *J* = 13.5 Hz, minor), 2.96 (d, *J* = 14 Hz, 2H), 3.26 (d, *J* = 13 Hz, minor), 3.41 (d, *J* = 12.5 Hz, 2H), 3.81 (d, *J* = 13 Hz, 2H), 4.06 (d, *J* = 13 Hz, minor), 4.51 (m, 4H), 4.58 (m, minor), 4.68 (d, *J* = 14 Hz, minor), 5.21 (d, *J* = 9 Hz, 2H), 5.59 (d, *J* = 8 Hz, minor); ^{13}C NMR (75 MHz, $CDCl_3$)

δ: 21.3, 22.2, 23.4, 23.5, 24.4, 24.7, 27.4, 28.3, 28.5, 29.9, 43.0, 43.6, 45.9, 46.7, 48.5, 48.7, 49.6, 49.8, 79.2, 79.3, 155.7, 171.5, 173.0; IR (KBr): 3403, 3326, 2961, 2931, 2868, 2860, 1710, 1658, 1628, 1531, 1452, 1436, 1390, 1366, 1244, 1172, 1047; HRMS calcd. for $C_{29}H_{52}N_4NaO_6$ m/z 575.3779, found m/z 575.3796.

Synthesis of **4**

To a well stirred solution of Boc and benzyl protected bispidine compound **A3** (0.295 g, 0.935 mmol) in methanol (10 mL) was added few drops of acetic acid and 10% of Pd/C (0.029 g) and kept under positive pressure of H_2 gas. Stirred the reaction mixture for 8h at room temperature. The reaction mixture was filtered and evaporated in *vacuo* to obtain the amine. The obtained amine was dissolved in DCM and trifluoroacetic acid (0.715 mL, 9.35 mmol), stirred for 2 h at room temperature. The reaction mixture was evaporated and used as such for further reaction. The obtained amine was added to the DCM solution containing tert-butyloxy carbonyl (Boc) protected Ala (0.353 g, 1.87 mmol), NHS (0.258 g, 2.24 mmol), DCC (0.460 g, 2.24 mmol) and NEt_3 (0.31 mL, 2.24 mmol). The resultant solution was stirred for 24 h at room temperature. After completion of reaction, the reaction mixture was evaporated and re-dissolved in ethyl acetate and the filtrate was washed with 0.2N H_2SO_4, saturated aq. $NaHCO_3$ and water. The organic layer was collected and dried over anhyd. Na_2SO_4 and evaporated under vacuum to obtain the crude product, which was purified by column chromatography (Ethyl acetate/Hexane in 4:6) to give 0.390 g compound **4** as a solid.

In the ^1H NMR spectrum in $CDCl_3$, compound **4** showed signals for major and minor conformers. We have mentioned the signals for minor conformer wherever possible.^{13}C NMR also showed

signal for minor conformer, therefore more ^{13}C peaks are observed in the ^{13}C spectrum of compound **4**.

Yield: 89%. Mp: 166 -168 ºC;

$[\alpha]_D^{21}$ = -77º (c 0.05, methanol);

^1H NMR (400 MHz, $CDCl_3$) δ: 1.16 – 1.27 (d, *J* = 7.2 Hz, major + minor, 6H), 1.41 (s, 18H), 1.50 (minor), 1.90 (m, 2H), 1.93 (minor), 1.99 (minor), 2.12 (m, 2H), 2.86 (minor d, *J* = 13.6 Hz), 2.94 (d, *J* = 13.6 Hz, 2H), 3.27 (minor d, *J* = 13.2 Hz), 3.40 (d, *J* = 12.8 Hz, 2H), 3.86 (d, *J* = 12.8 Hz, 2H), 4.04 (minor d, *J* = 12.8 Hz), 4.50 (m, 2H), 4.58 (d, *J* = 13.6 Hz, 2H), 4.72 (minor d, *J* = 13.6 Hz), 5.38 (d, *J* = 8 Hz, 2H), 5.74 (minor d, *J* = 8 Hz); ^{13}C NMR (125 MHz, $CDCl_3$) δ: 18.8, 19.7, 27.6, 28.3, 28.6, 30.4, 32.2, 45.8, 46.2, 46.6, 49.8, 50.0, 79.37, 79.43, 155.1, 155.4, 171.4, 172.4; IR (KBr): 3423, 3327, 2981, 2931, 2868, 1688, 1640, 1533, 1368, 1296, 1174, 1057; HRMS calcd. for $C_{23}H_{40}N_4NaO_6$ m/z 491.2840, found m/z 491.2824.

Methods: -

1. **Scanning electron microscopy:**

Sample solution for the imaging was made by dissolving the 1 mg of the compound in 1 ml of the solvent. A drop of the sample solution was placed on the glass slide allowed to dry in the air and coated with 10nm of gold. All the samples were analyzed using scanning electron microscope ZEISS EVO 50.

2. **Atomic force microscopy:**

A solution of compound (1mg/ml) was prepared in the solvent of choice. A drop of the sample solution was placed on the silicon wafer and allowed to dry in the air. All the sample were analyzed using Bruker Dimension Icon atomic force microscope. Nanoscope 5.31r software was used to analyze the data.

3. **Transmission Electron Microscopy (TEM):**

Samples for TEM were prepared by dissolving the compound in methanol. About 5µl aliquot of the sample solution was placed on a 200 mesh copper grid and allowed dry. Imaging was done using a TECHNAI G2 (20S-TWIN) electron microscope.

4. **Confocal Microscopy:**

Rhodamine was mixed with the sample prepared in methanol and vortexed for 30 seconds. About 20µl of the sample was drop cast on 20*60 mm slides and allowed to dry. Excess dye was removed by washing the slides with MilliQ water thrice. The slide was allowed to dry and used for imaging. Epifluorescence imaging was done in UV filter using 1.40 UPlanSApo 100x objective in Olympus IX51 epifluorescence microscope model. Slides were prepared similarly for confocal microscopy. Confocal images were captured using Olympus FV1200 microscope at UPlanSApo 100xo objective (λ at 540nm for Rhodamine B stained vesicles and λ at 515 nm for Nile Red stained vesicles). The step size in z-stacking was kept at 100 nm. Images were captured at 12.5µs/pixel frame rate. Cellsens software was used to construct 3D view of the z-stack of vesicles.

5. **Fluorescence spectrometer:**

All the steady-state fluorescence experiments were carried out on the Horiba Scientific Fluoromax-4 Spectrofluorometer. Fluorescence measurements were carried out by using 1 cm quartz cuvettes and the temperature was maintained at 25 ^{o}C.

6. **Cytotoxicity Assay in RAW264.7 cells:**

The resazurin assay was used to analyze the peptide's cytotoxicity profile. Stock concentration: 0.15 mg/ml, Working concentration: 0.03 mg/ml. After 24 hours of compound treatment media was removed and 20µl of 0.15mg/ml resazurin was added to 80 µl serum free media. This was incubated at 37^{0}C in 5% CO_2 for 20 minutes. And the reading was taken at 560/590 nm in MultiSkan Go.

7. **DOSY experiments:**

The experiments were performed on a 500 MHz Bruker Avance III HD spectrometer with a BBFO probe. A standard method with stimulated echo and LED using bipolar gradient pulses is utilized here to calculate the diffusion constant. The length of the gradient pulse(p30) is calibrated (1.2 ms) to obtain a 98% decay in the signal on increasing the gradient strength(gpz6) using 1D DOSY pulse sequence. The value of diffusion time (d20) allowed during the pulse sequence is 0.06 s. 32 transients in t1-dimension were recorded with linear increase in the gradient strength using 2D DOSY pulse sequence. The diffusion constants were fitted using Bruker standard Relaxation analysis tool.

8. **Cellular uptake of Rhodamine mixed with 2:**

Rhodamine (5µg/ml) labeled compound was used to treat RAW264.7 cells (on coverslip) for 24 hours. Washed twice with 1X PBS. Prepared slides and imaged in Olympus Confocal FV1200 microscope at 60x magnification (LUCPLFLN lens). Fluorescence of Rhodamine was observed using a 543 nm laser.

9. **Cellular uptake of FITC-tagged peptide (CorTS1(LRRLRLRRNRL-NH_2) - Corneal Targeting Sequence 1)[2]:**

Seeded ~25000 RAW264.7 cells in 35 mm Petri dishes containing 19 mm coverslips and allowed cells to grow for 24 hours at 37^{0}C in 5% CO_2 in DMEM containing 10% FBS and 1% Penstrep. After 24 hours, washed once in 1X PBS and treated the petri dishes as follows for 24 hours:

i. CONTROL – No compound, No CorTS1, No rhodamine in serum-free DMEM
ii. DYE CONTROL – No compound, no CorTS1, rhodamine dye (5µg/ml) in serum-free DMEM
iii. PEPTIDE CONTROL – No compound, CorTS1 (10µM), No dye in serum-free DMEM
iv. PEPTIDE DYE CONTROL – No Compound, CorTS1 (10µM), Rhodamine dye (5µg/ml) in serum-free DMEM
v. 200 µg/ml compound, CorTS1 (10µM), Rhodamine dye (5µg/ml) in serum-free DMEM

After 24 hours washed with 1X PBS twice, prepared slides, and captured images in Olympus Confocal FV1200 microscope at 60x magnification using 473 nm, and 543 nm laser.

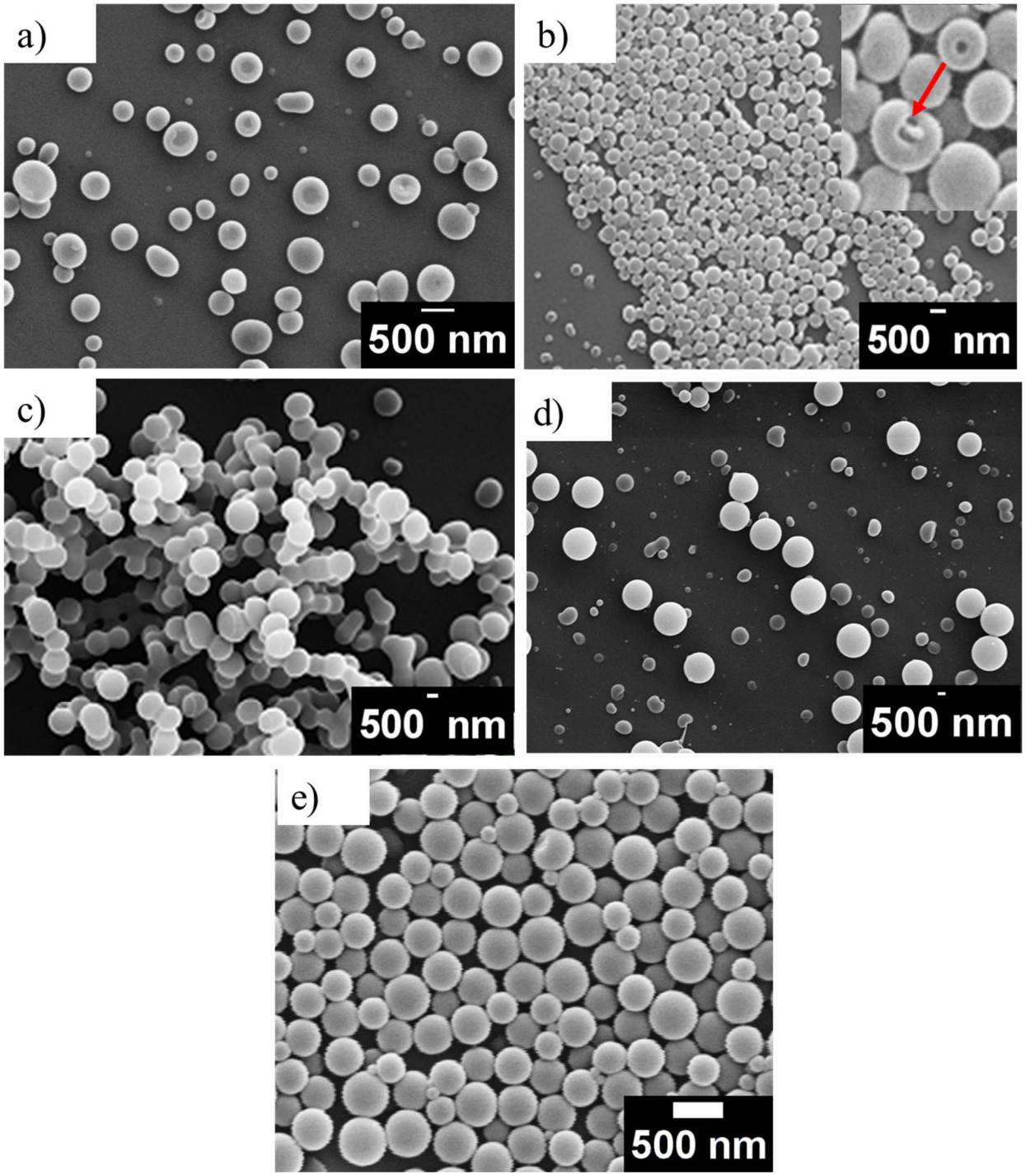

Figure S1. (a) SEM image of **1** (concentration: 0.476 mM) (b) SEM image of **1** (concentration: 0.715 mM) (c) SEM image of **1** (concentration: 2.14 mM) (d) SEM image of (**1** + 0.02 equivalents of Rhodamine B dye) compound **1** with 1.43 mM concentration was used. (e) SEM image of **1** (concentration: 1.43 mM) in 1:1 (water: ethanol) mixture showing vesicular self-assembly.

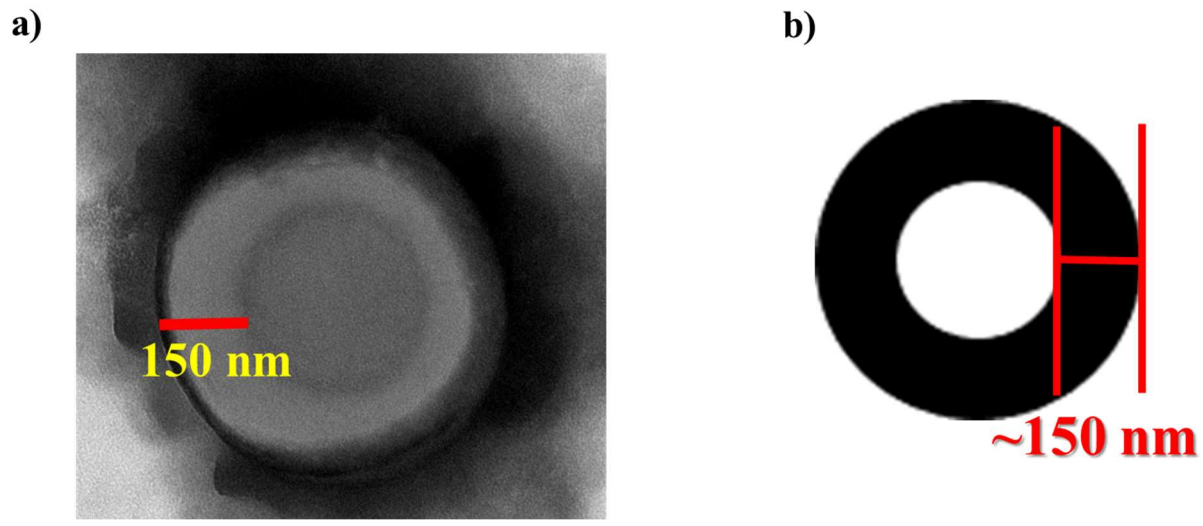

Figure S2. (a) TEM image of **1** in 1mg/ml. The scale bars indicate the wall thickness of vesicles. (b) Cartoon representation of vesicle indicating thickness of wall. The sample was stained with a negative stain by using phosphotungstic acid for 1 minute.

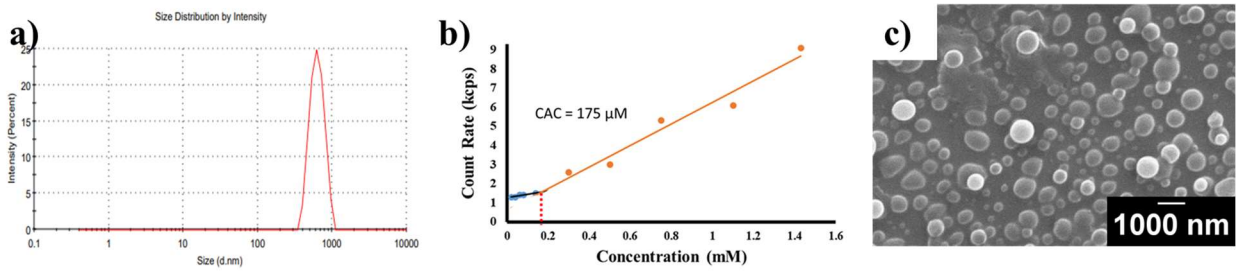

Figure S3. (a) Dynamic light scattering of **1** in 1mg/ml (b) CAC of **1** calculated from DLS (c) SEM image of **2** in 10 % methanol and water.

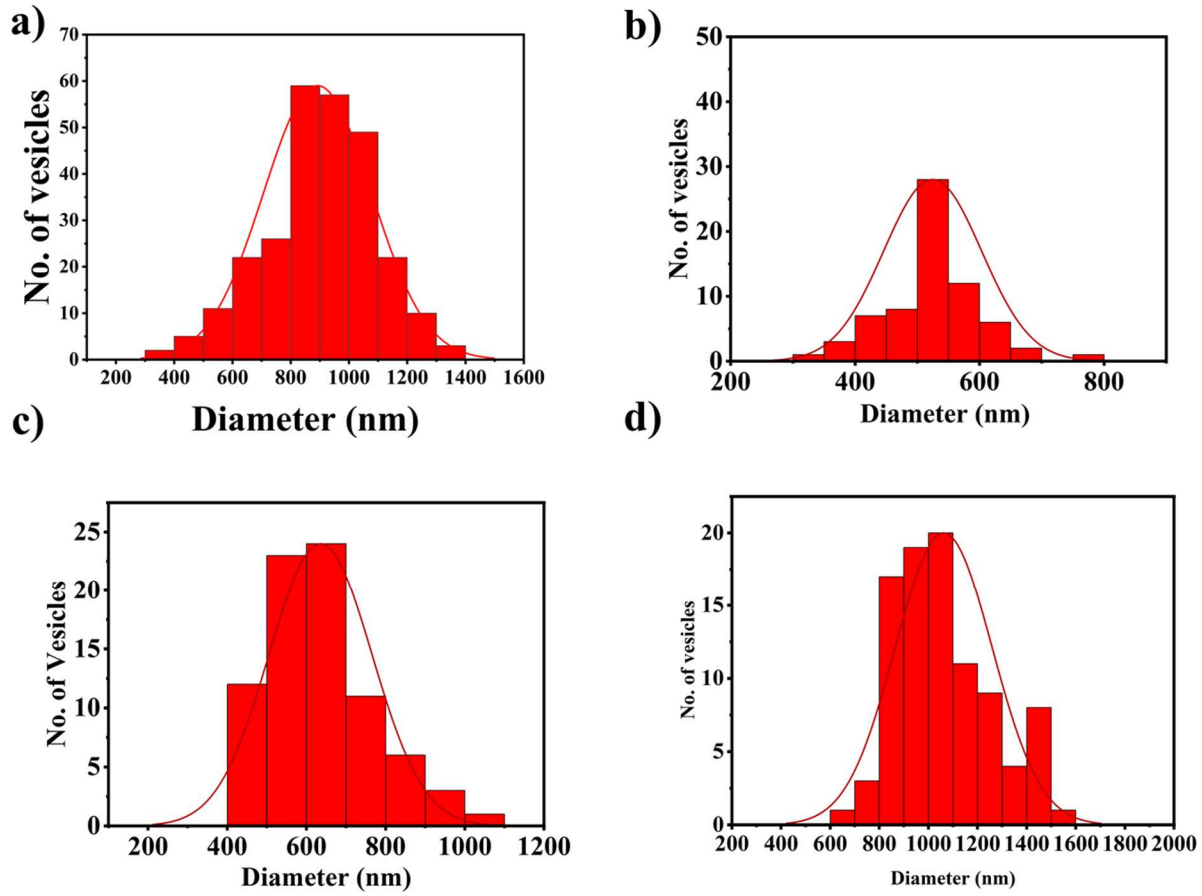

Figure S4. Histogram based on SEM images (a) Size distributions of diameters of vesicles at 1 mg/ml of **1** (b) Size distribution of diameters of vesicles at 1 mg/ml of **2** in 10 % of methanol and water. (c) Size distributions in diameters of vesicles at 1 mg/ml of **3** (c) Size distribution of diameters of vesicles at 1 mg/ml of **4**.

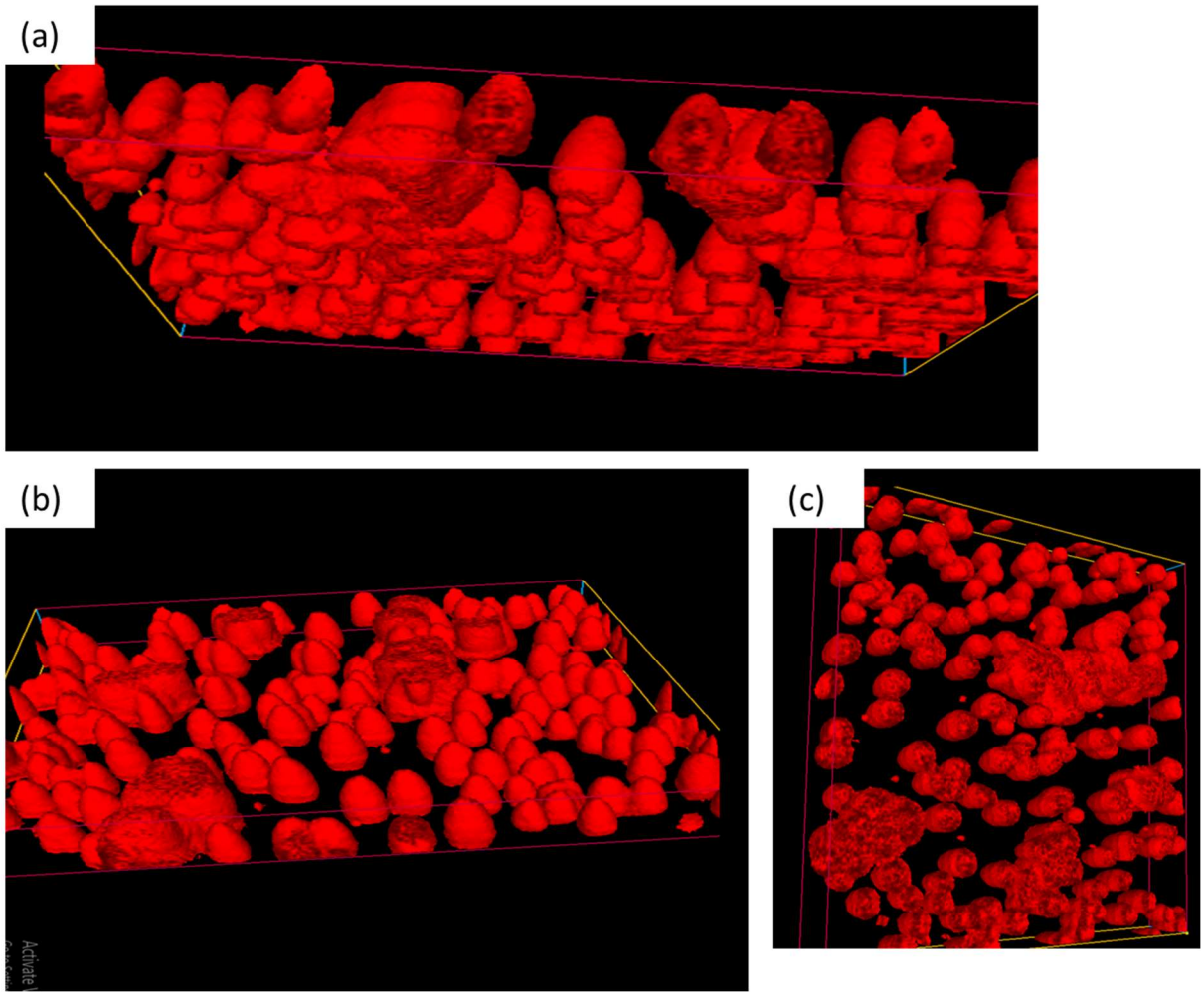

Figure S5. Side view of 3D confocal microscopy at 100x Objective (5x zoomed image) of **1** + 0.02 equivalents of Rhodamine B dye at λ_{ex} at 540 nm (a) side view (b) Top view (c) Bottom view constructed using Olympus Cellsens software. Step size=100nm, Z ~ 4µm.

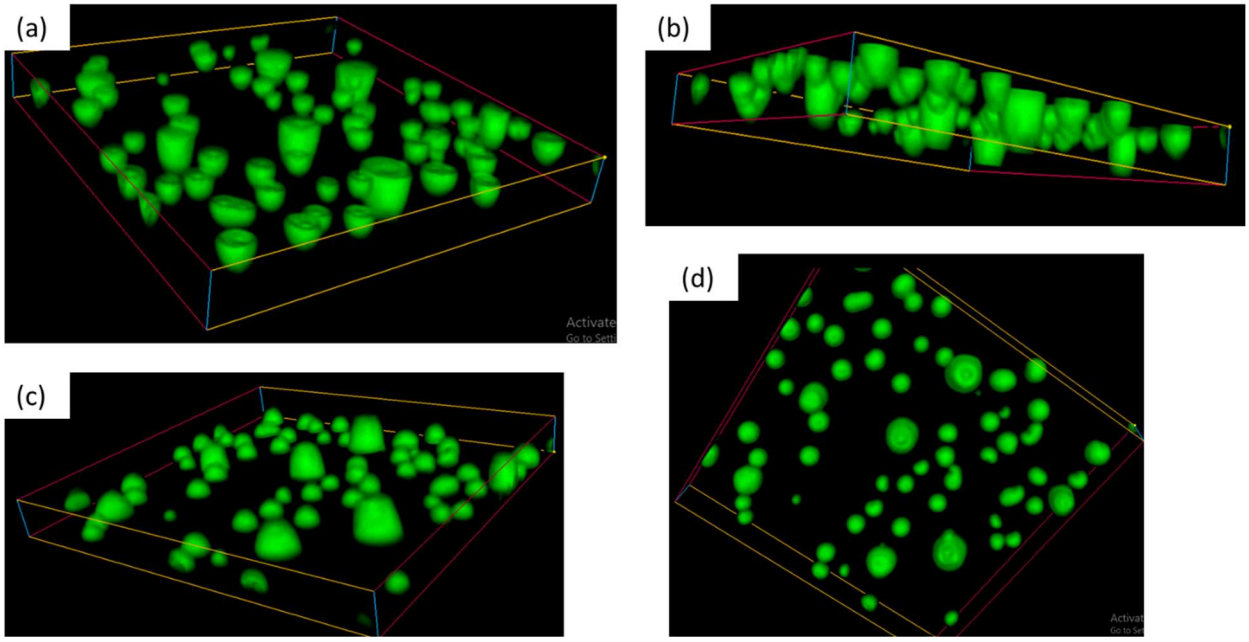

Figure S6. (a) Bottom face view of 3D confocal microscopy at 100x objective (5x zoomed image) of **1** + 0.02 equivalents of Nile Red dye at λ_{ex} at 515 nm (b) Side view (c) Top view (d) Top side view constructed using Olympus Cellsens software. Step size=100nm, Z ~ 4µm.

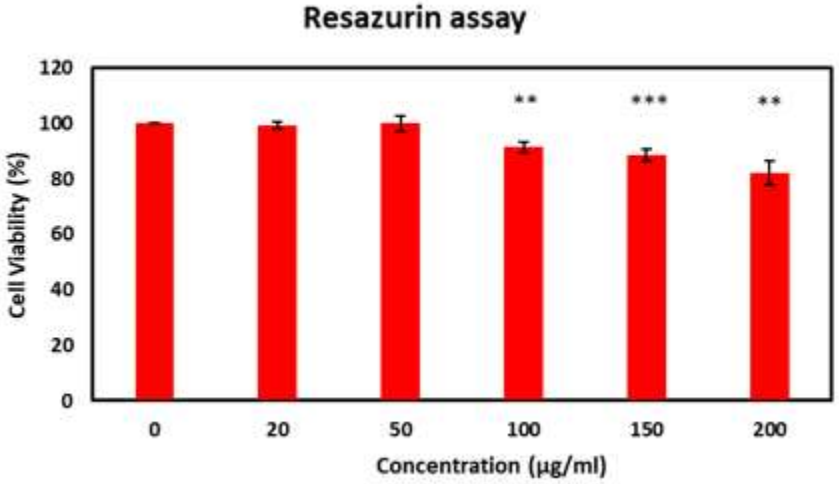

Figure S7. Cell Viability profile of **2** for RAW264.7 cells. Cells were incubated with various concentrations (0, 20, 50, 100, 150, and 200µg/ml) of the compound for 24 h followed by 20-minute incubation with Resazurin (in serum-free media). Untreated cells act as control (n=3±std dev) 2-tailed unpaired t-test was conducted to check the significance of the difference between control and compound treatments.

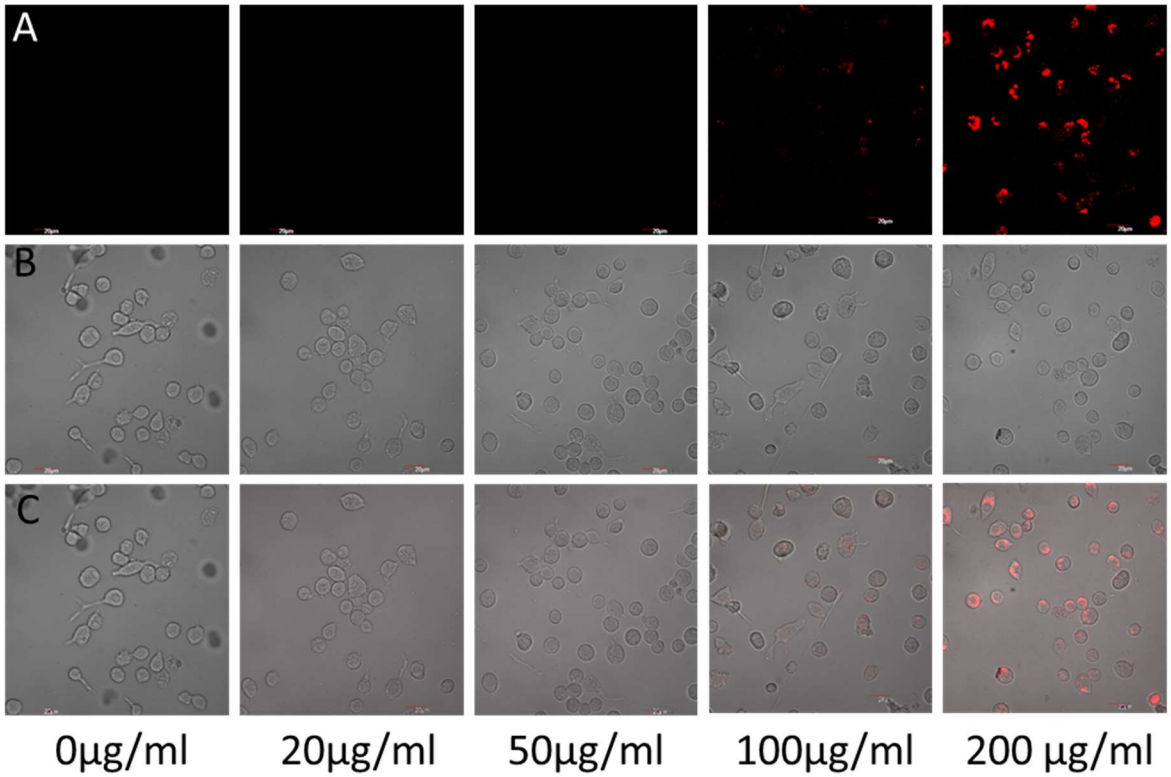

Figure S8. Representative confocal microscopy images of RAW264.7 cells treated with the Rhodamine B along with **2**. **A** Fluorescent image, **B** DIC image, and **C** DIC-Fluorescence merge image. Cells were incubated with various concentrations (0, 20, 50, 100 and 200 µg/ml) of the rhodamine along with **2** for 24 h followed by PBS washing and Imaging in Olympus Confocal FV1200 microscope at 60 x magnification (scale bar = 20 µm).

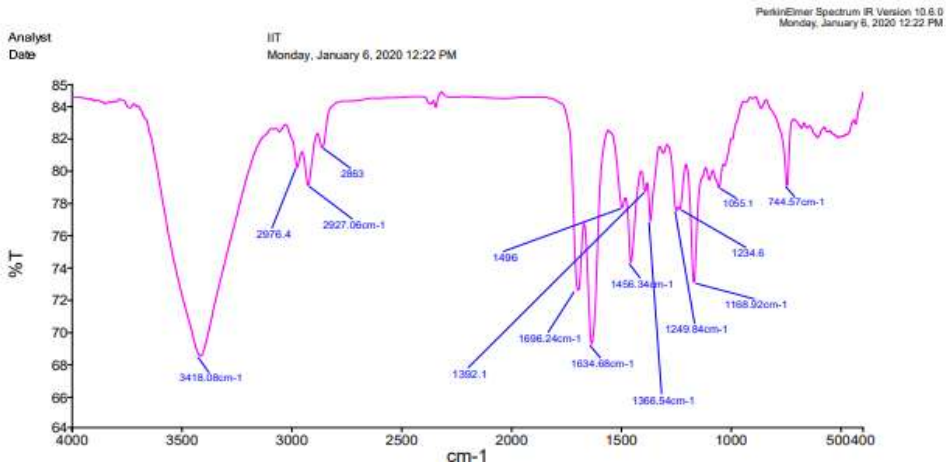

Figure S9. The FT-IR spectrum of **1** showed strong bands at 3418 cm^{-1} and 1634 cm^{-1} (amide I), and 1696 cm^{-1} indicating β-strand arrangement.

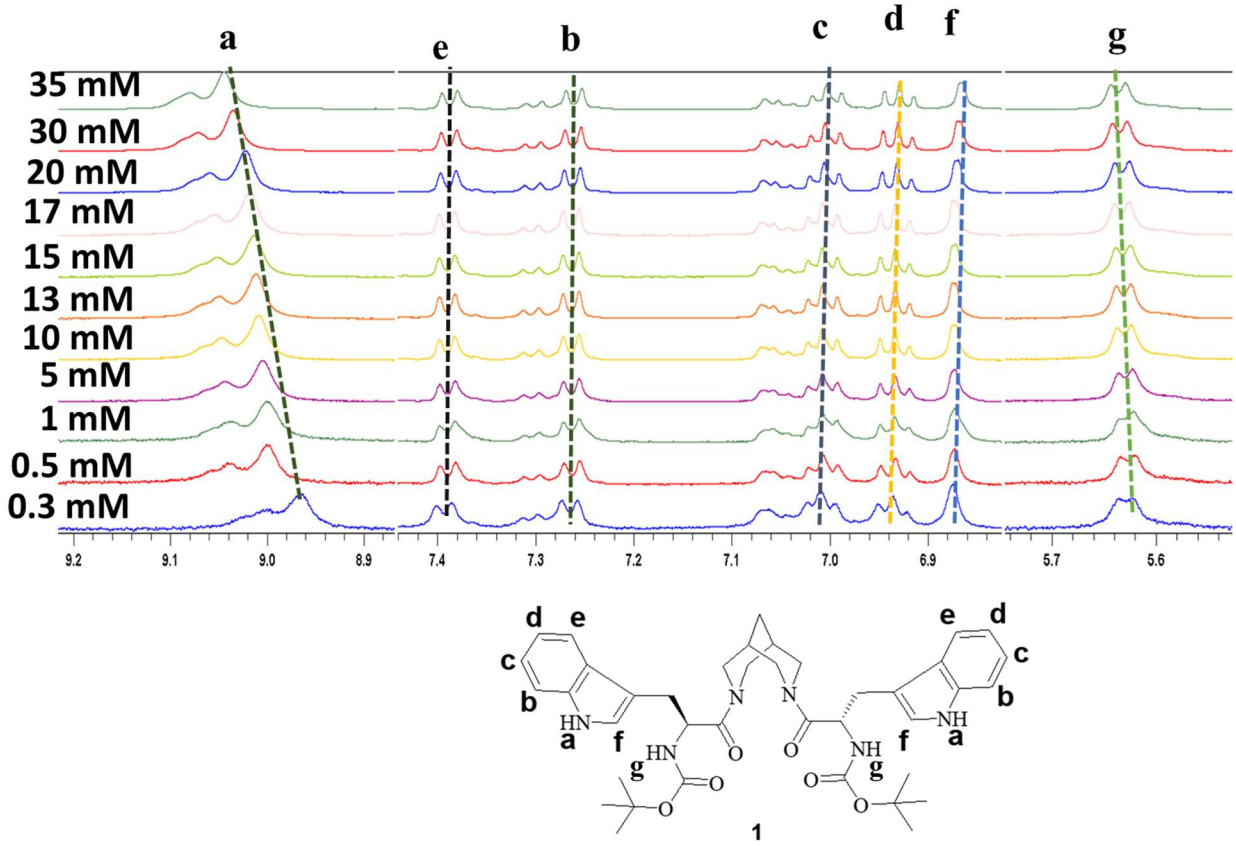

Figure S10. Concentration dependent study of **1**. Concentration is mark on the left side of each spectrum. Selected protons are marked on the structure and spectra. All spectra were recorded on 500 MHz NMR at 25 ºC in CD_3CN.

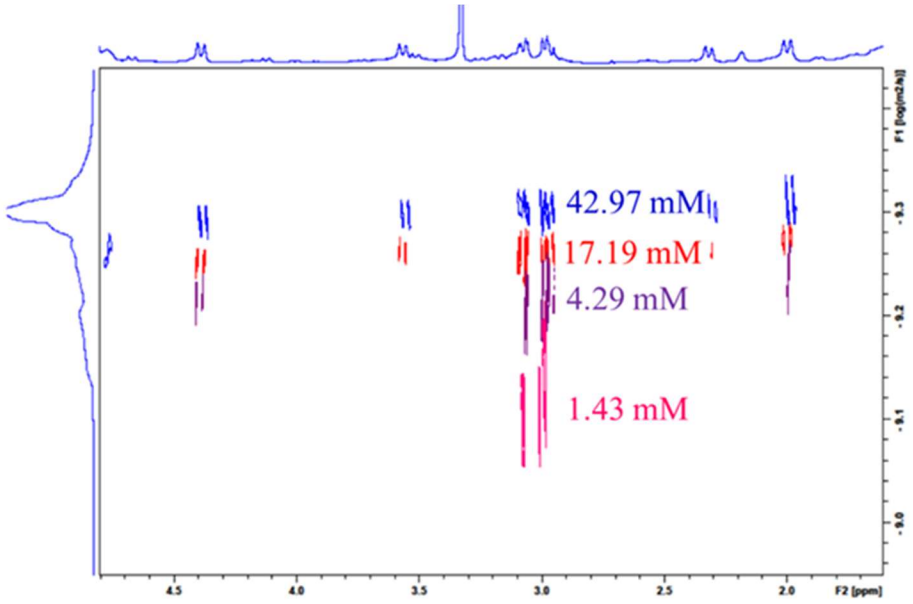

Region (PPM)	1.43 mM	4.29 mM	17.19 mM	42.97 mM
	Unit: m^2/s			
3.028-2.945	7.79×10^{-10}	6.33×10^{-10}	5.55×10^{-10}	4.96×10^{-10}

Figure S11. Diffusion constant from DOSY of **1** at different concentration in CD_3OD.

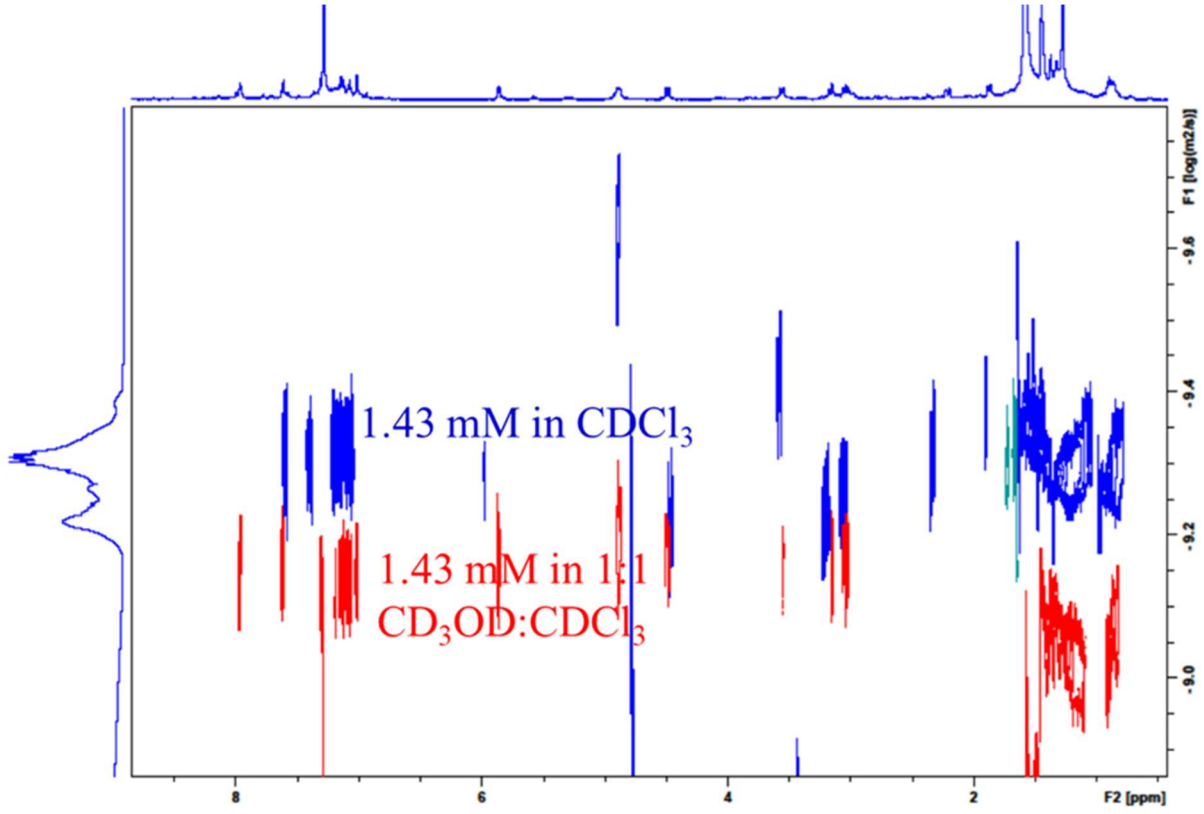

Region	1:1 MeOD:$CDCl_3$ (Unit: m^2/s)	$CDCl_3$ (Unit: m^2/s)
7.080-7.059	4.77×10^{-10}	7.19×10^{-10}

Figure S12. Comparison between the diffusion constant of compound **1** in 1:1 CD_3OD: $CDCl_3$ and only $CDCl_3$ at 1.43 mM concentration from DOSY experiment.

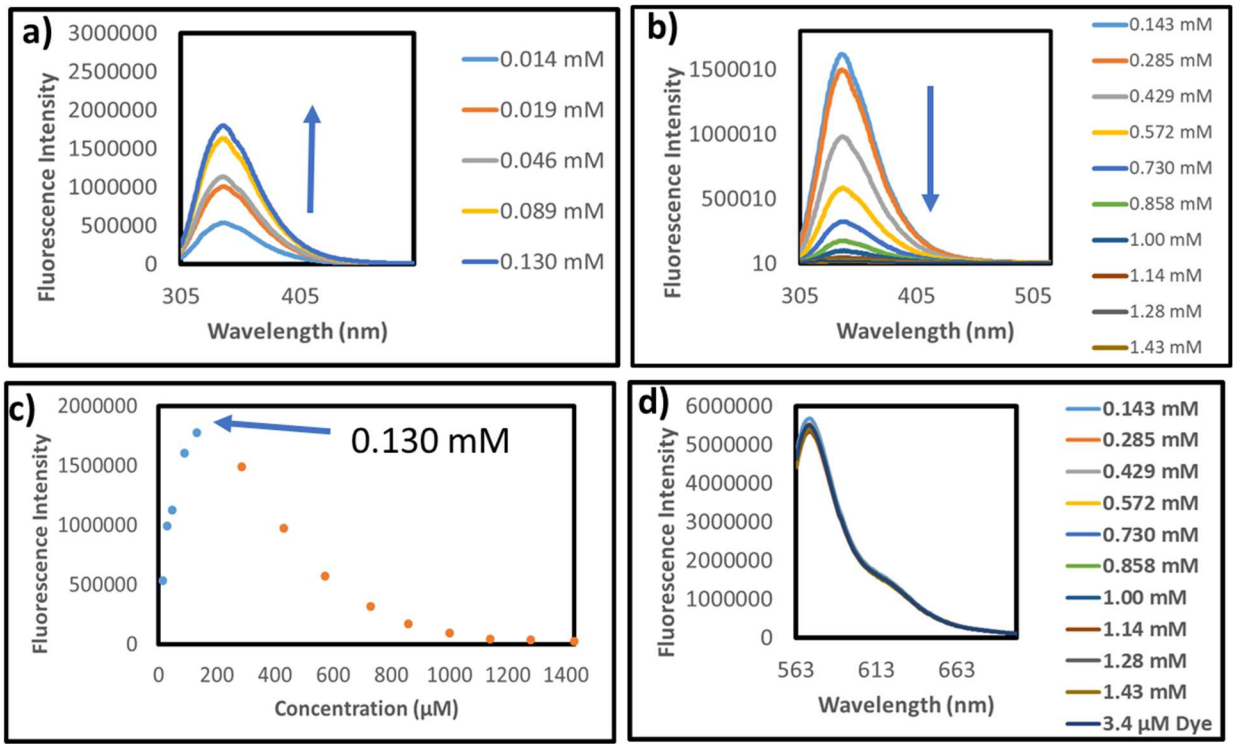

Figure S13. a) Concentration-dependent fluorescence spectra of **1** in concentration range of 14 - 130 µM in methanol (λ_{ex} at 295 nm). (b) Concentration-dependent fluorescence spectra of **1** in concentration range of 143 -1430 µM in methanol (λ_{ex} at 295 nm). (c) Plot of fluorescence emission intensity at 343 nm vs concentration of **1** (d) Fluorescence spectra of Rhodamine B dye alone and with addition of different concentrations of **1** in methanol (λ_{ex} at 553 nm).

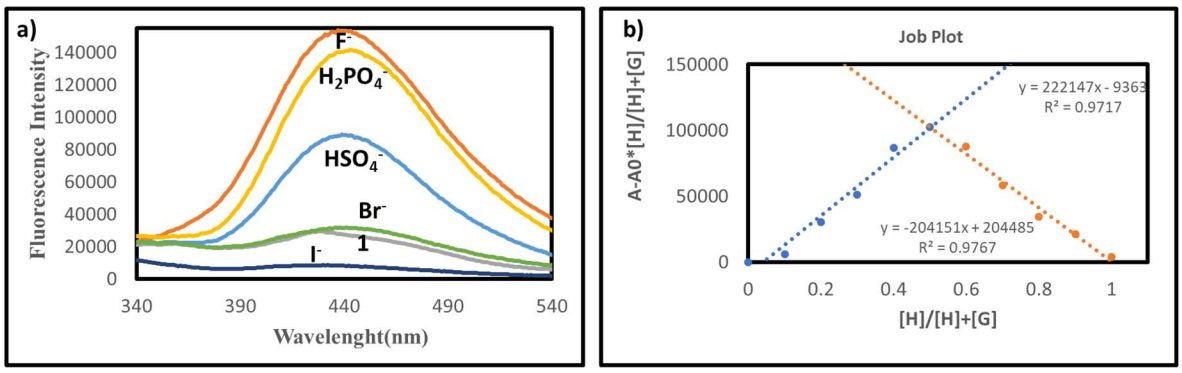

Figure S14. (a)Binding study of anions with **1** (b) Job Plot of $H_2PO_4^-$ titration against **1**.

Table S1. Chemical shift deviations of **1-4.**

Compound	Proton	δ (obs)	δ (random coil)	Chemical shift deviation i.e. Δδ(CHα) = δ(CHα) (obs) – δ (random coil)
1	Trp (CHα)	4.88 ppm	4.70 ppm	0.18 ppm
2	Trp (CHα)	4.89 ppm	4.70 ppm	0.18 ppm
3	Leu (CHα)	4.52 ppm	4.17 ppm	0.35 ppm
4	Ala (CHα)	4.50 ppm	4.35 ppm	0.15 ppm

Table S2. Crystal data and structure refinement for 1 (CCDC 2172117).

Identification code	BW2
Empirical formula	$C_{39}H_{52}N_6O_7$
Formula weight	716.884
Temperature/K	273.15
Crystal system	monoclinic
Space group	$P2_1$
a/Å	13.650(13)
b/Å	9.887(10)
c/Å	15.827(16)
α/°	90
β/°	112.53(3)
γ/°	90
Volume/Å^3	1973(3)
Z	2
ρ_{calc}g/cm^3	1.207
μ/mm^{-1}	0.084
F(000)	768.4
Crystal size/mm^3	0.25 × 0.08 × 0.10
Radiation	Mo Kα (λ = 0.71073)
2Θ range for data collection/°	3.36 to 50
Index ranges	$-14 \leq h \leq 18$, $-11 \leq k \leq 13$, $-19 \leq l \leq 17$
Reflections collected	11416
Independent reflections	5912 [R_{int} = 0.0544, R_{sigma} = 0.1647]
Data/restraints/parameters	5912/31/470
Goodness-of-fit on F^2	1.040
Final R indexes [I>=2σ (I)]	R_1 = 0.0736, wR_2 = 0.1509

Final R indexes [all data]	$R_1 = 0.1539$, $wR_2 = 0.1957$
Largest diff. peak/hole / e Å^{-3}	0.29/-0.30
Flack parameter	-2.3(18)

Table S3. Crystal data and structure refinement for 3 (CCDC 2172115).

Identification code	BL2
Empirical formula	$C_{29}H_{52}N_4O_6$
Formula weight	552.760
Temperature/K	273.15
Crystal system	monoclinic
Space group	$P2_1$
a/Å	6.6858(4)
b/Å	26.2740(17)
c/Å	11.3518(7)
α/°	90
β/°	102.219(3)
γ/°	90
Volume/Å^3	1948.9(2)
Z	2
ρ_{calc}g/cm^3	0.942
μ/mm^{-1}	0.066
F(000)	604.3
Crystal size/mm^3	0.22 × 0.09 × 0.13
Radiation	Mo Kα (λ = 0.71073)
2Θ range for data collection/°	3.1 to 56.64
Index ranges	$-8 \leq h \leq 8$, $-35 \leq k \leq 35$, $-15 \leq l \leq 15$
Reflections collected	64410

Independent reflections	9644 [R_{int} = 0.0739, R_{sigma} = 0.0494]
Data/restraints/parameters	9644/37/363
Goodness-of-fit on F^2	0.989
Final R indexes [I>=2σ (I)]	R_1 = 0.0505, wR_2 = 0.1282
Final R indexes [all data]	R_1 = 0.1138, wR_2 = 0.1644
Largest diff. peak/hole / e $Å^{-3}$	0.16/-0.18
Flack parameter	-0.8(4)

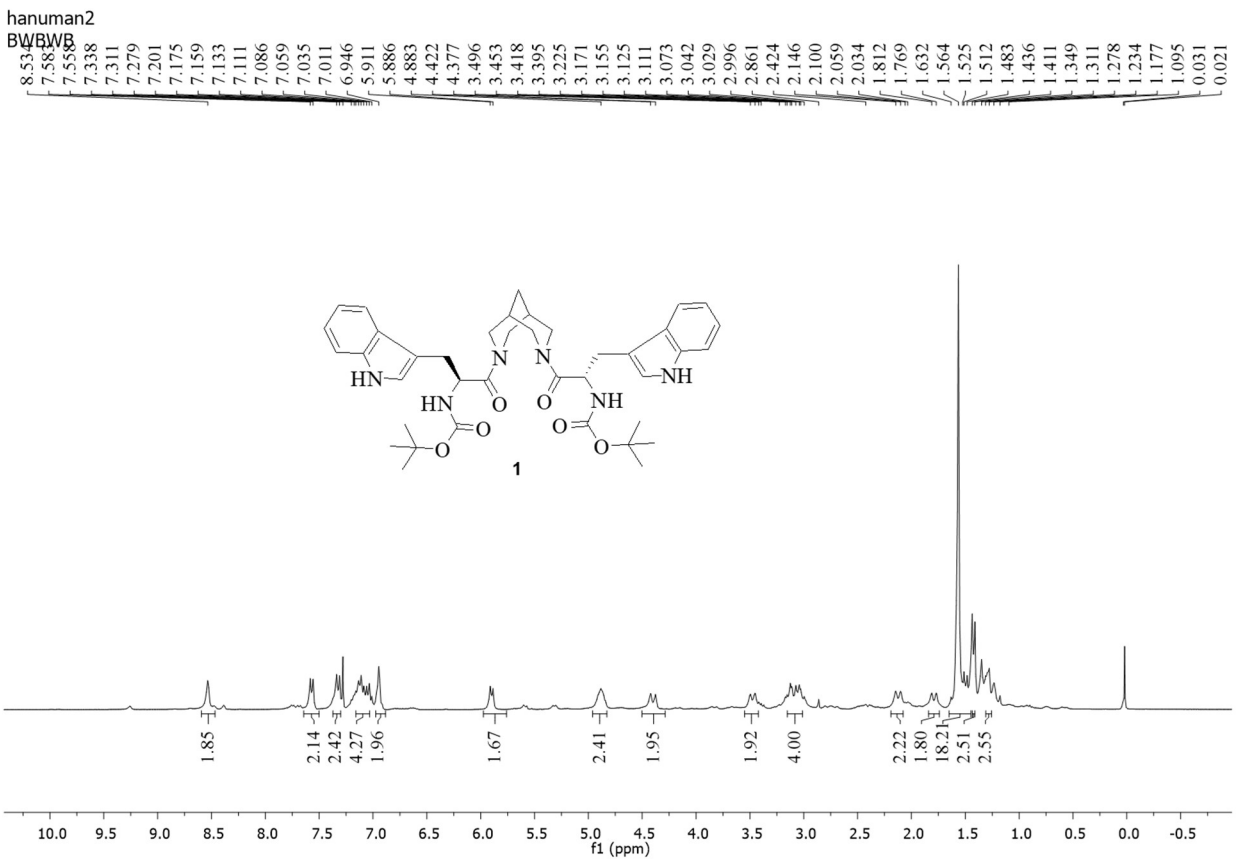

1

^{1} H NMR ($CDCl_3$, 300 MHz) of **1**

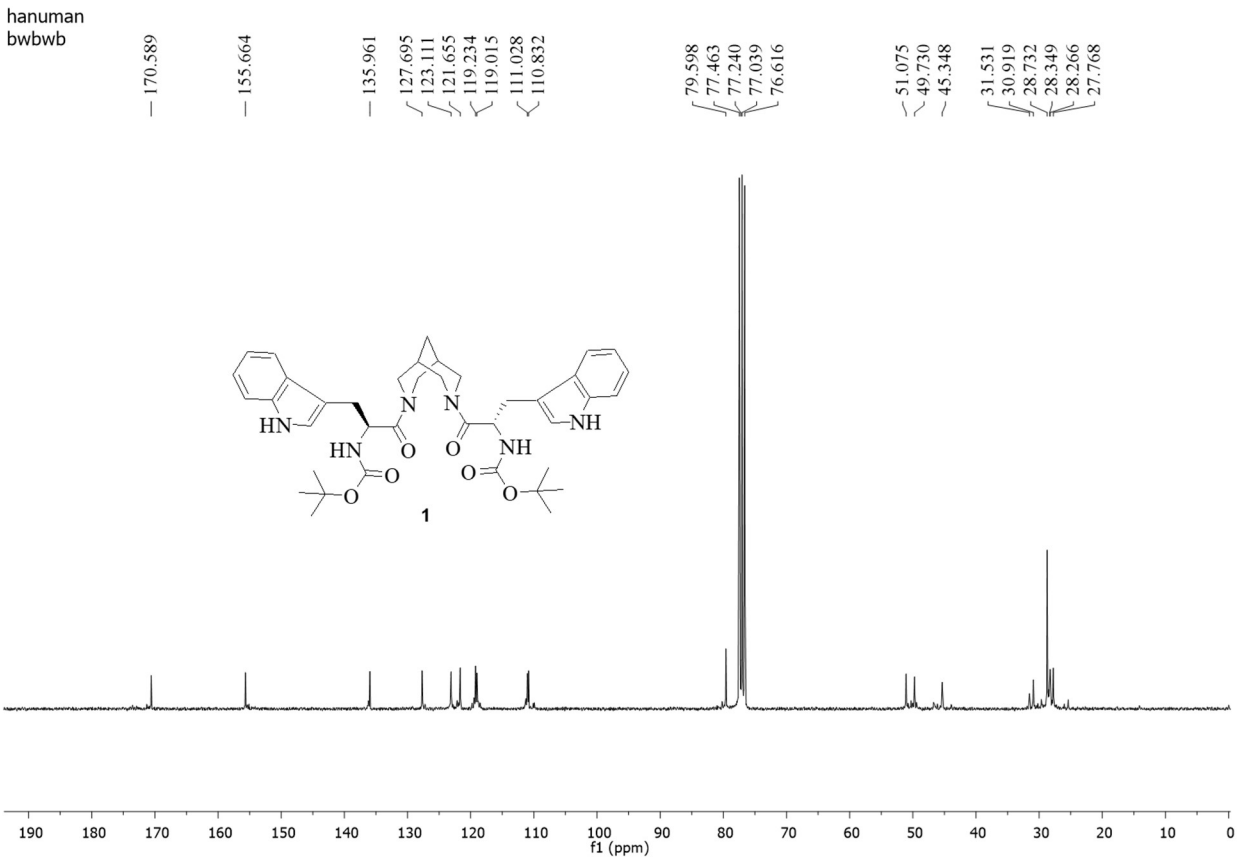

^{13}C NMR ($CDCl_3$, 75MHz) of **1**

Mass Spectrum SmartFormula Report

Analysis Info

Analysis Name	Z:\Data\FEBRUARY 2019\dwbwb000003.d	Acquisition Date	2/19/2019 2:53:37 PM
Metnod	tune_wide.m	Operator	IISc-MBU
Sample Name	tm 1:100	Instrument / Ser#	micrOTOF-Q 10262
Comment			

Acquisition Parameter

Source Type	ESI	Ion Polarity	Positive	Set Nebulizer	14.5 psi
Focus	Active	Set Capillary	4500 V	Set Dry Heater	330 °C
Scan Begin	50 m/z	Set End Plate Offset	-500 V	Set Dry Gas	4.0 l/min
Scan End	3000 m/z	Set Collision Cell RF	400.0 Vpp	Set Divert Valve	Source

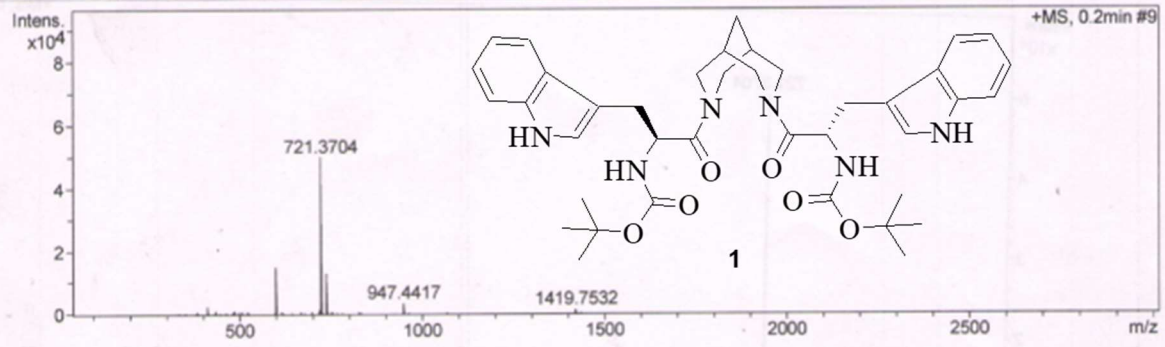

Meas. m/z	#	Formula	m/z	err [ppm]	Mean err [ppm]	rdb	N-Rule	e⁻ Conf	mSigma	Std I	Std Mean m/z	Std I VarNorm	Std m/z Diff	Std Comb Dev
721.3704	1	C 39 H 50 N 6 Na O 6	721.3684	-2.8	-1.6	17.5	ok	even	76.68	0.1217	0.0018	0.0395	0.0029	0.8427

HRMS of **1**

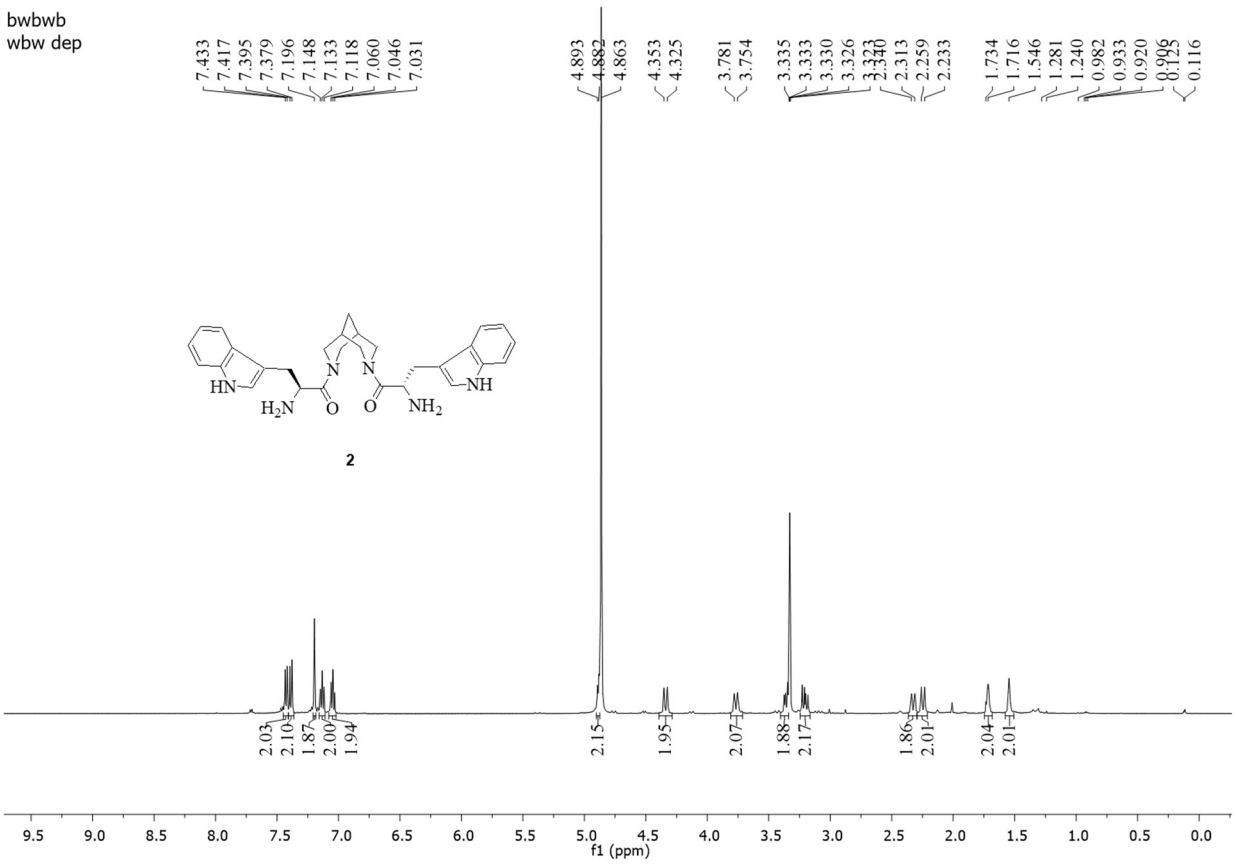

2

^{1} H NMR (CD_3OD, 500 MHz) of **2**

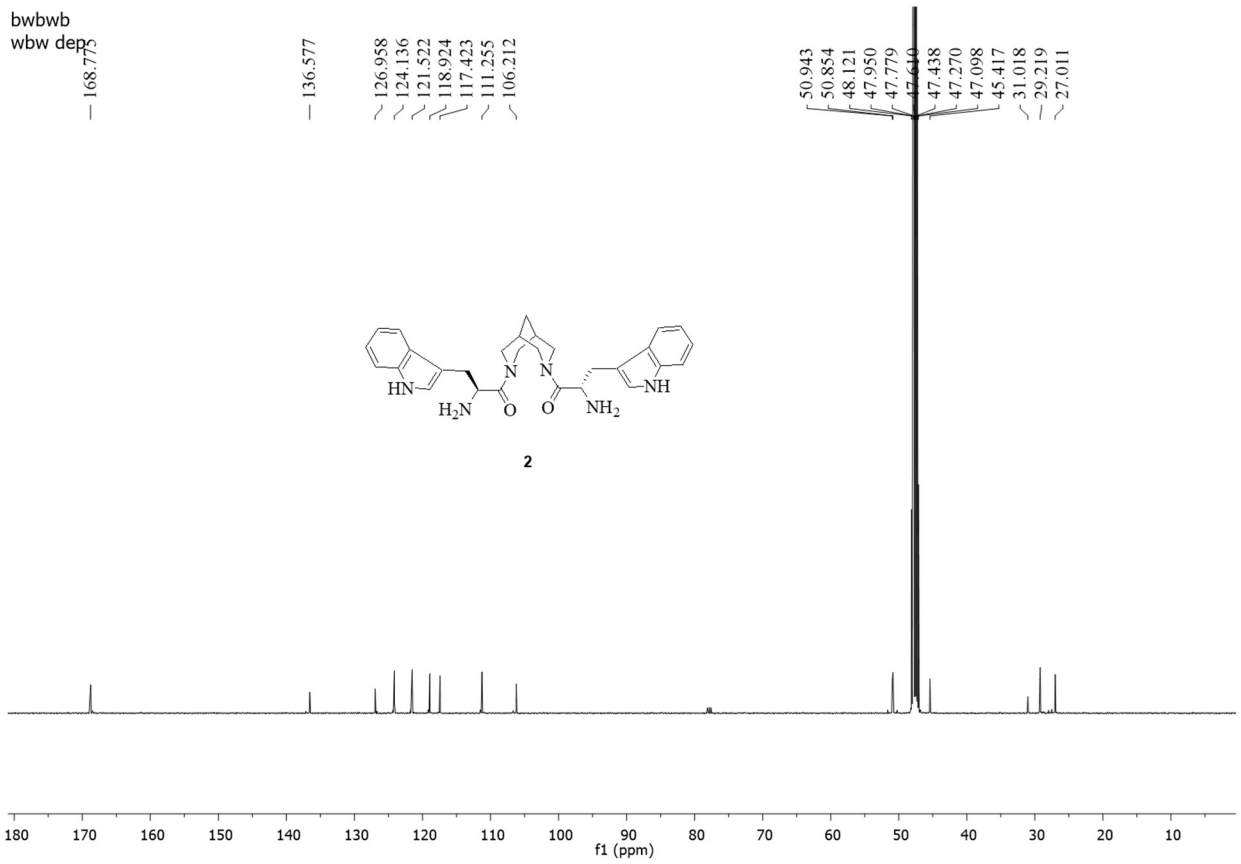

^{13}C NMR (CD_3OD, 125 MHz) of **2**

Mass Spectrum SmartFormula Report

Analysis Info

Analysis Name	Y:\Data\DEC 2021\vh r 5000001.d	Acquisition Date	12/23/21 3:18:39 PM
Method	tune_wide.m	Operator	BDAL@DE
Sample Name	tm 1 100	Instrument	micrOTOF-Q 228888.10262
Comment			

Acquisition Parameter

Source Type	ESI	Ion Polarity	Positive	Set Nebulizer	0.4 Bar
Focus	Active	Set Capillary	4500 V	Set Dry Heater	180 °C
Scan Begin	300 m/z	Set End Plate Offset	-500 V	Set Dry Gas	4.0 l/min
Scan End	3000 m/z	Set Collision Cell RF	700.0 Vpp	Set Divert Valve	Source

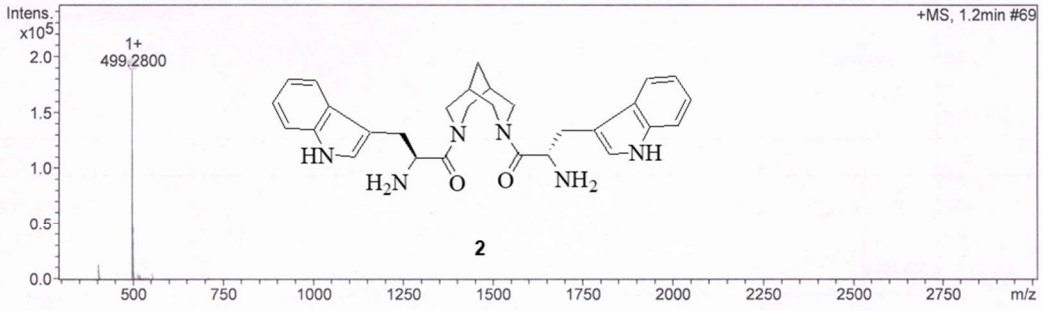

Meas. m/z	#	Ion Formula	m/z	err [ppm]	Mean err [ppm]	rdb	N-Rule	e⁻ Conf	mSigma	Std I	Std Mean m/z	Std I VarNorm	Std m/z Diff	Std Comb Dev
499.279983	1	C29H35N6O2	499.281601	3.2	7.7	15.5	ok	even	28.3	49.1	n.a.	n.a.	n.a.	n.a.

HRMS of **2**

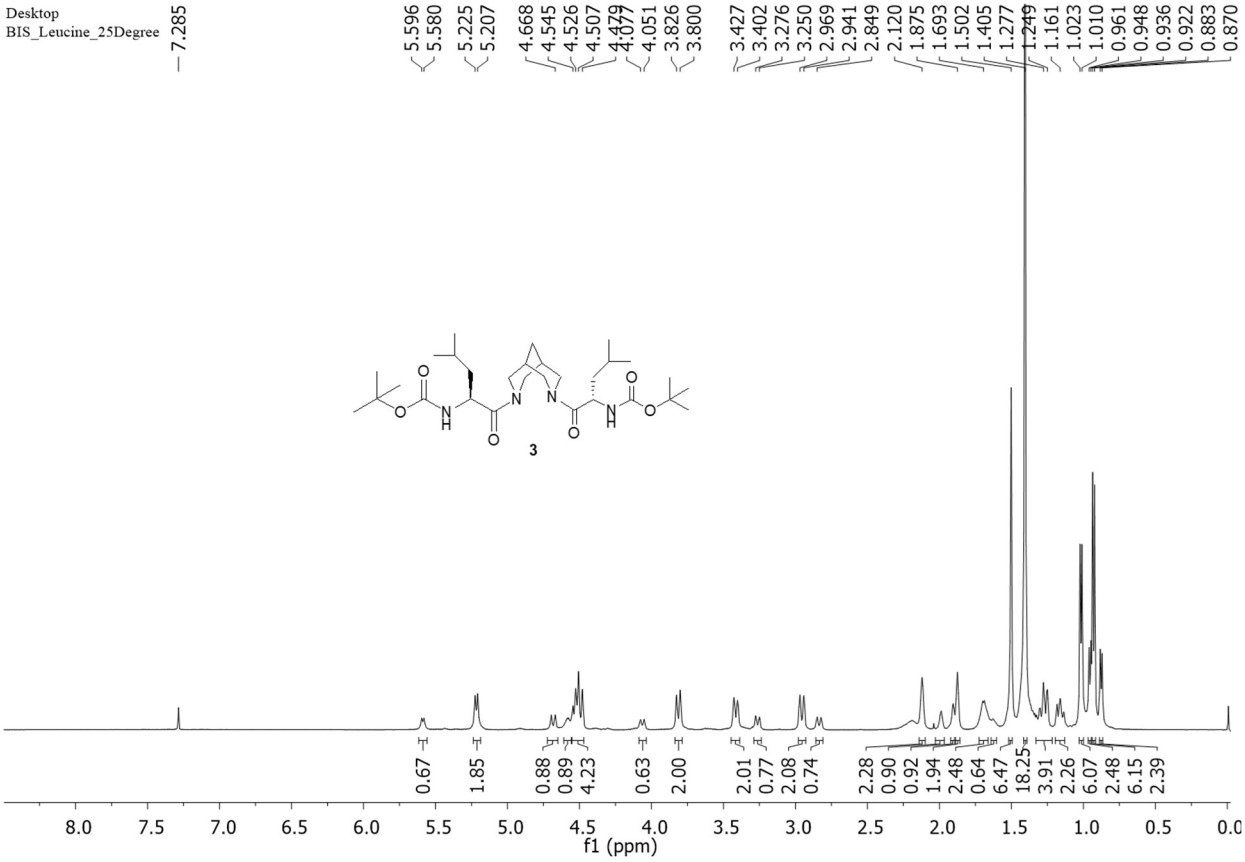

^{1} H NMR ($CDCl_3$, 500 MHz) of **3**

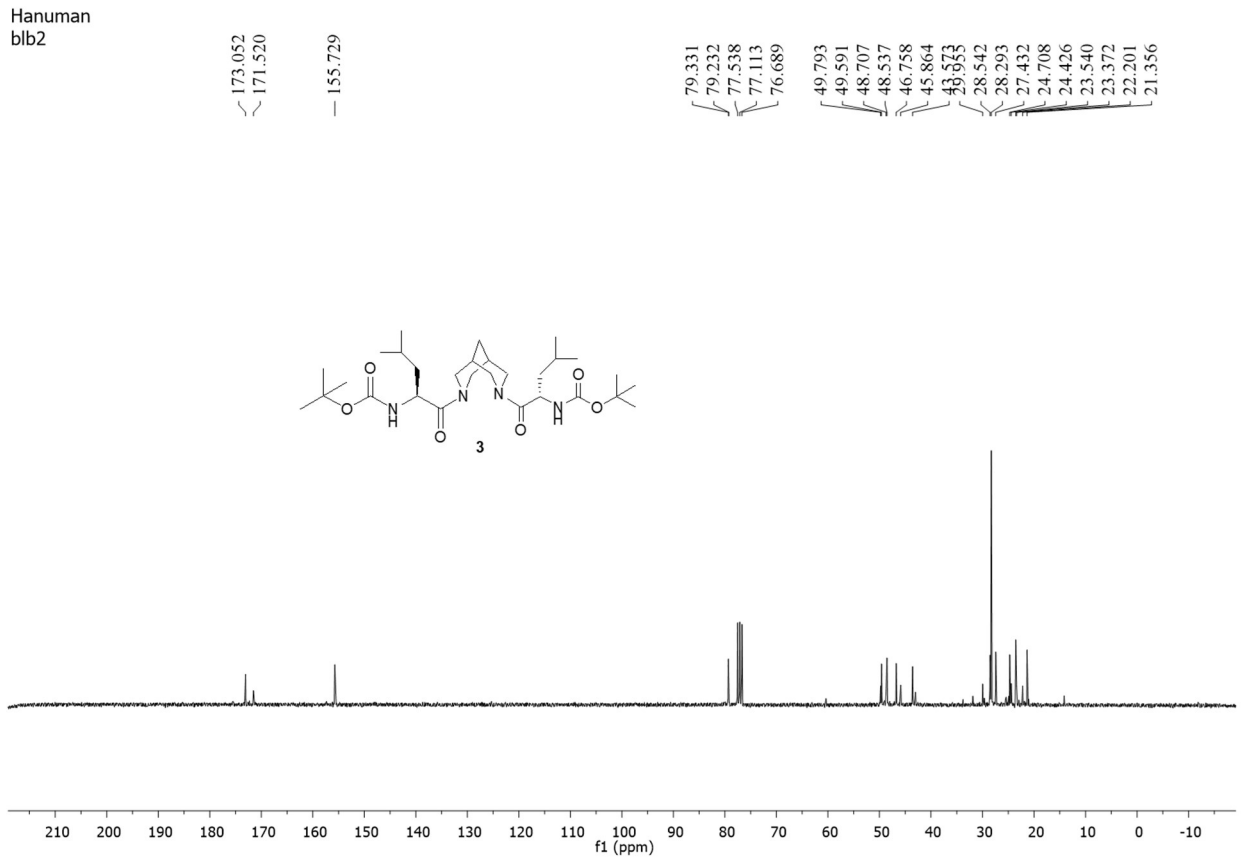

^{13}C NMR ($CDCl_3$, 75MHz) of **3**

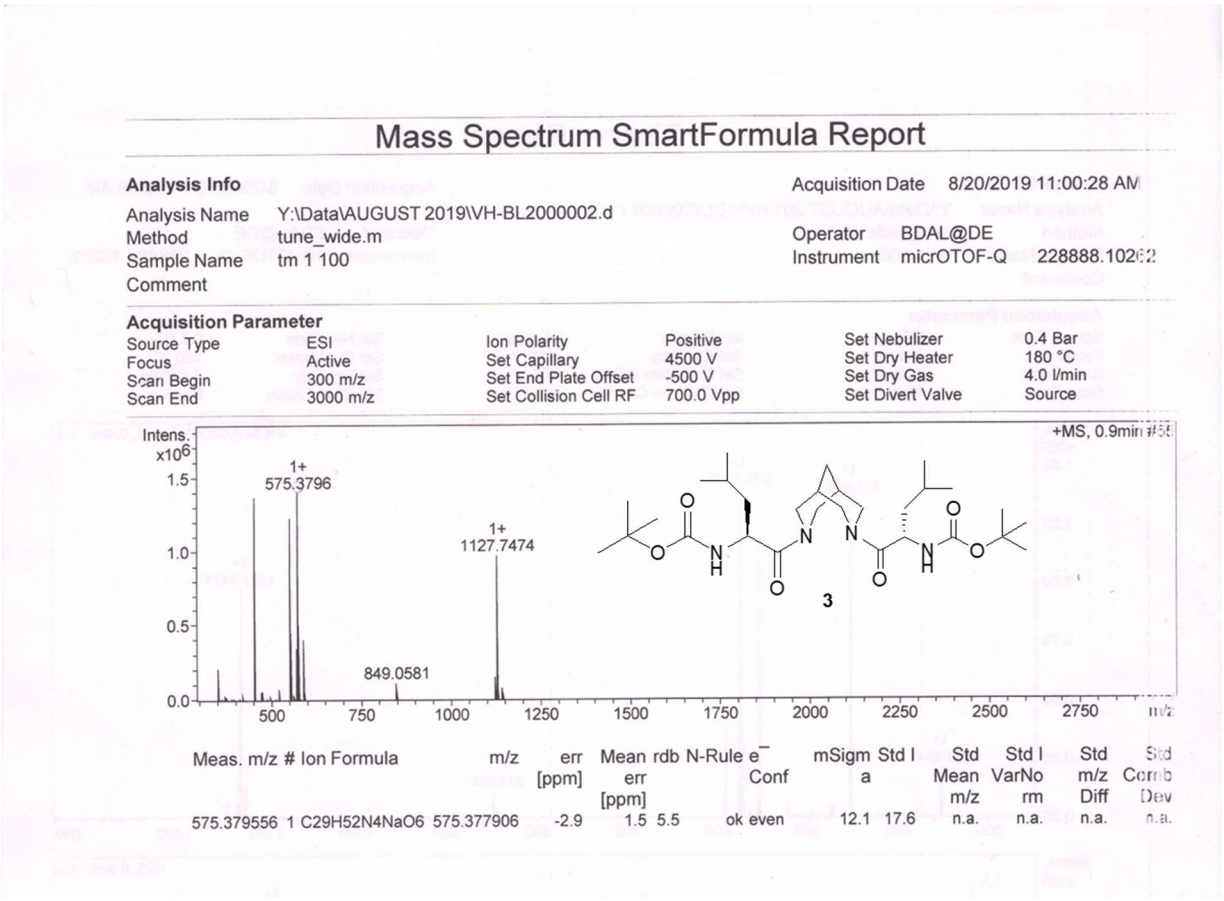
Mass Spectrum SmartFormula Report
Analysis Info
Acquisition Date 8/20/2019 11:00:28 AM
Analysis Name Y:\Data\AUGUST 2019\VH-BL2000002.d
Method tune_wide.m
Sample Name tm 1 100
Comment
Operator BDAL@DE
Instrument micrOTOF-Q 228888.10262
Acquisition Parameter
Source Type ESI
Focus Active
Scan Begin 300 m/z
Scan End 3000 m/z
Ion Polarity Positive
Set Capillary 4500 V
Set End Plate Offset -500 V
Set Collision Cell RF 700.0 Vpp
Set Nebulizer 0.4 Bar
Set Dry Heater 180 °C
Set Dry Gas 4.0 l/min
Set Divert Valve Source
Intens.
x10^6
1.5
1.0
0.5
0.0
1+
575.3796
1+
1127.7474
849.0581
+MS, 0.9min
500
750
1000
1250
1500
1750
2000
2250
2500
2750
m/z
3
Meas. m/z # Ion Formula m/z err [ppm] Mean err [ppm] rdb N-Rule e⁻ Conf mSigma Std I Std Mean m/z Std I VarNorm Std m/z Diff Std Comb Dev
575.379556 1 C29H52N4NaO6 575.377906 -2.9 1.5 5.5 ok even 12.1 17.6 n.a. n.a. n.a. n.a.

HRMS of **3**

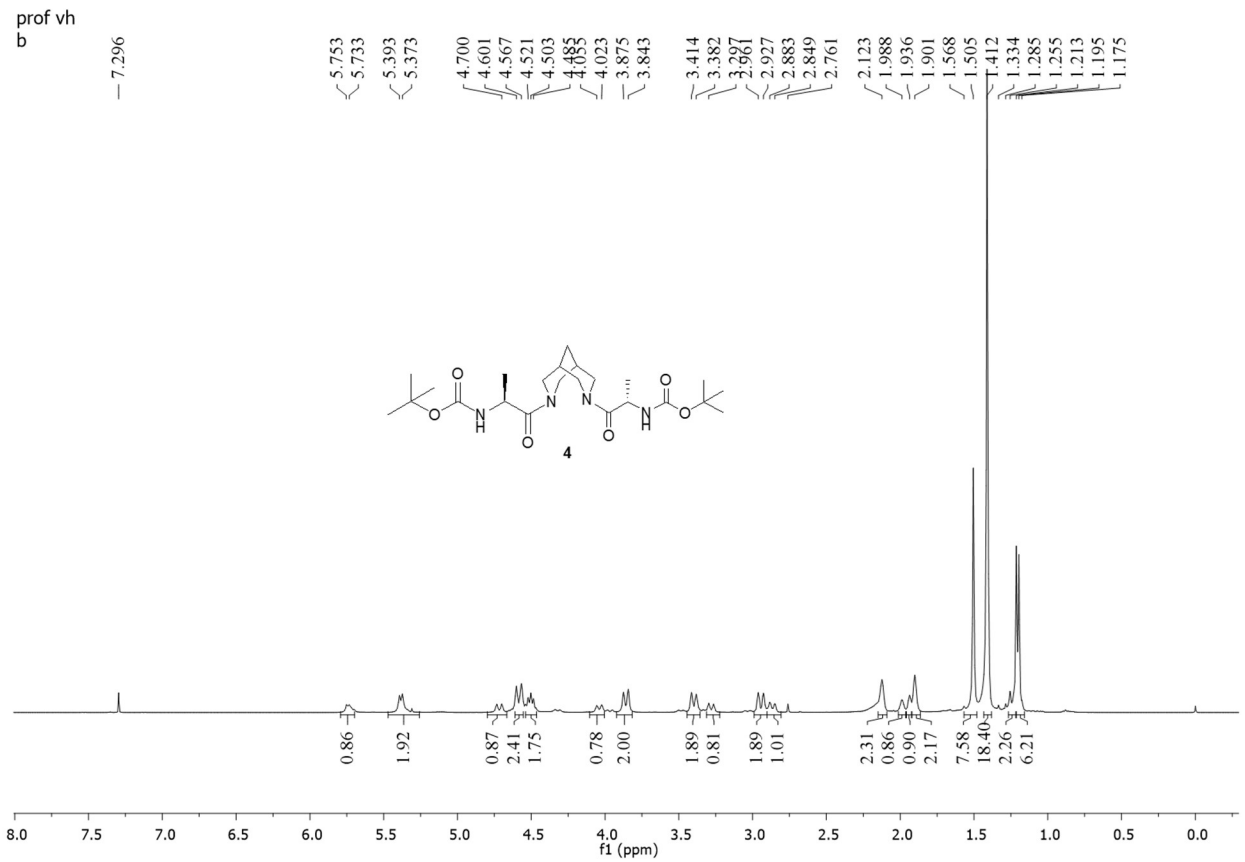

^{1} H NMR ($CDCl_3$, 400 MHz) of **4**

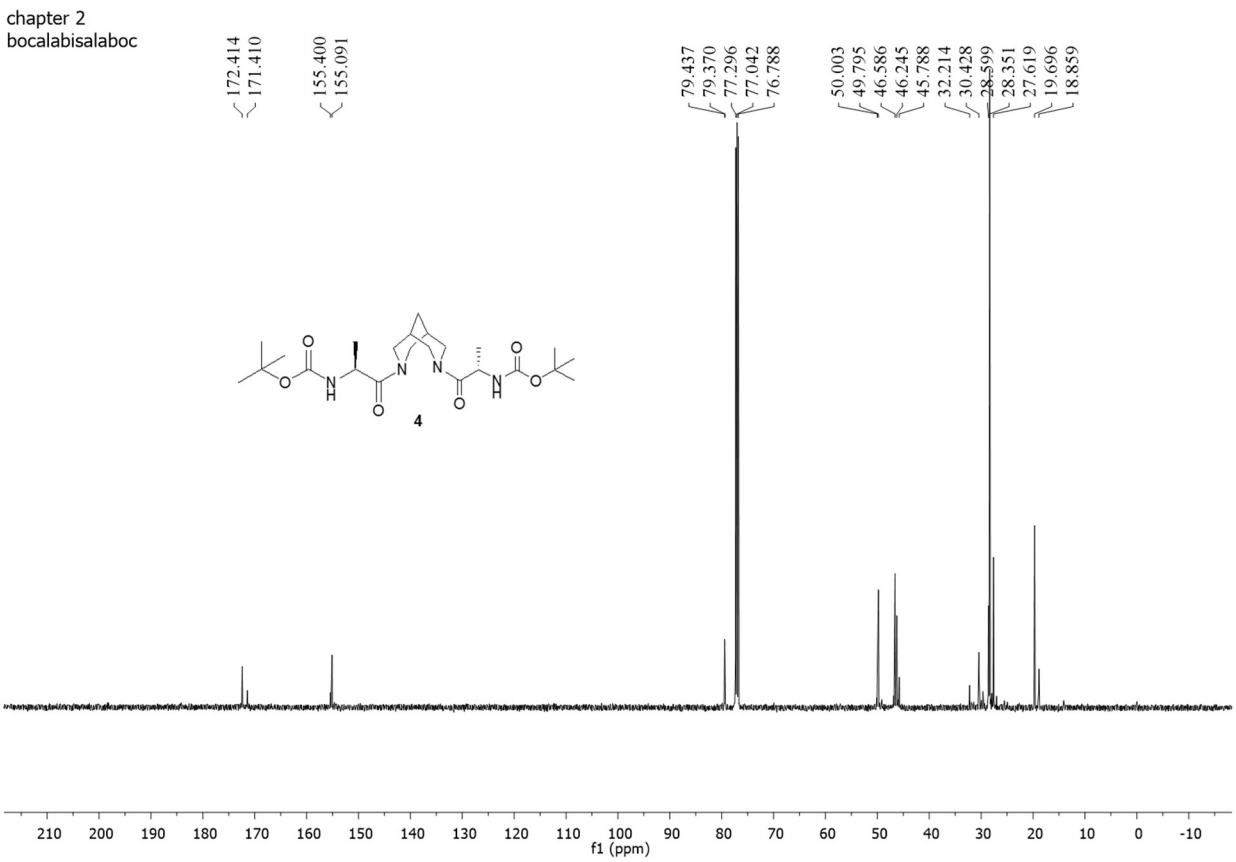

^{13}C NMR ($CDCl_3$, 100MHz) of **4**

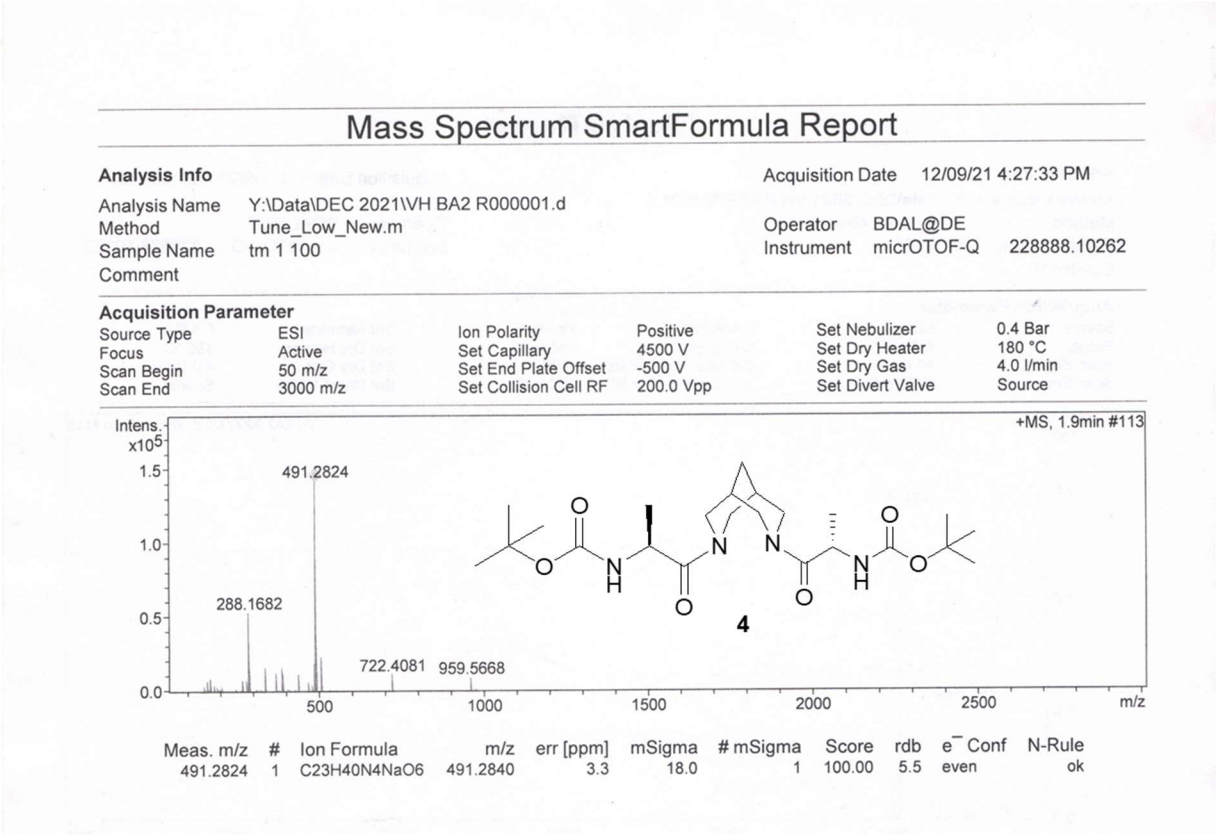
Mass Spectrum SmartFormula Report
Analysis Info
Acquisition Date 12/09/21 4:27:33 PM
Analysis Name Y:\Data\DEC 2021\VH BA2 R000001.d
Method Tune_Low_New.m
Sample Name tm 1 100
Comment
Operator BDAL@DE
Instrument micrOTOF-Q 228888.10262
Acquisition Parameter
Source Type ESI
Focus Active
Scan Begin 50 m/z
Scan End 3000 m/z
Ion Polarity Positive
Set Capillary 4500 V
Set End Plate Offset -500 V
Set Collision Cell RF 200.0 Vpp
Set Nebulizer 0.4 Bar
Set Dry Heater 180 °C
Set Dry Gas 4.0 l/min
Set Divert Valve Source
+MS, 1.9min #113
Intens.
x10^5
1.5
1.0
0.5
0.0
491.2824
288.1682
722.4081
959.5668
500
1000
1500
2000
2500
m/z
4
Meas. m/z # Ion Formula m/z err [ppm] mSigma # mSigma Score rdb e⁻ Conf N-Rule
491.2824 1 C23H40N4NaO6 491.2840 3.3 18.0 1 100.00 5.5 even ok

HRMS of **4**

==== Shimadzu LCsolution Analysis Report ====

C:\LabSolutions\Data\Project1\Background.lcdwbw11.lcd

Acquired by	: Admin
Sample Name	: wbw final1
Sample ID	: wbw final1
Tray#	: -1
Vail #	: -1
Injection Volume	: 20 uL
Data File Name	: Background.lcdwbw11.lcd
Method File Name	: Pushpendranew.lcm
Batch File Name	:
Report File Name	: Default.lcr
Data Acquired	: 1/1/2000 3:19:48 AM
Data Processed	: 1/1/2000 4:04:50 AM

<Chromatogram>

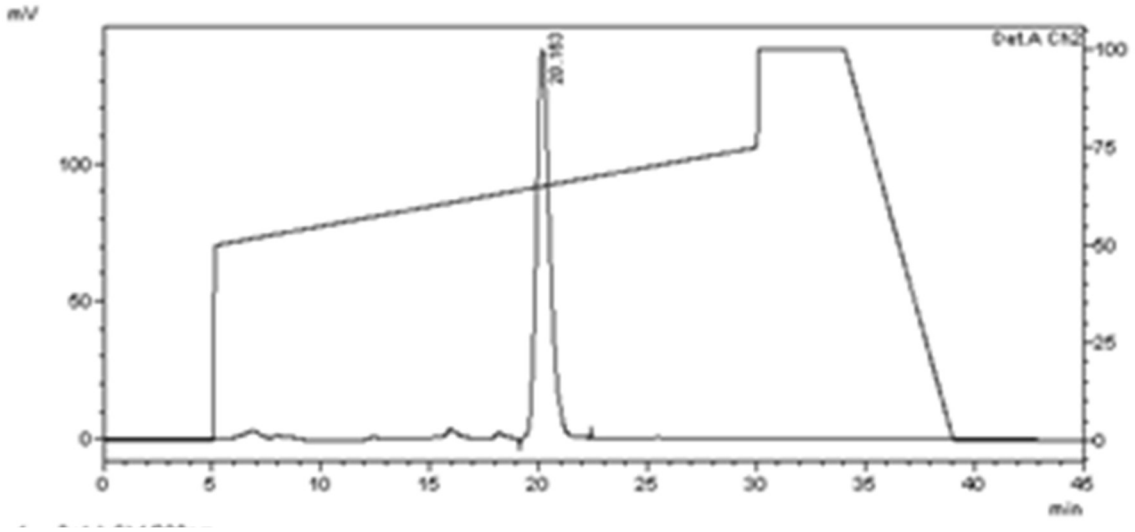

HPLC chromatogram of **1** in Solvent system ACN+TFA (0.1%) and H_2O+TFA (0.1%).

Reference

1. S. Juneja, H. Singh, S. Palui, S. Trivedi, S. S. Singh, V. Haridas and S. Pandey, *J. Phys. Chem. B*, 2019, **123**, 3112–3117.
2. S. Shankar, S. G. Shah, S. Yadav and A. Chugh, *European Journal of Pharmaceutics and Biopharmaceutics*, 2021, **166**, 216–226.